A 6-year AMSU-based climatology of upper-level troughs and associated precipitation distribution in the Mediterranean region

Beatriz M. Funatsu, C. Claud, Jean-Pierre Chaboureau

A 6-year AMSU-based climatology of upper-level troughs and associated precipitation distribution in the Mediterranean region

B. M. Funatsu,[1] C. Claud,[1] and J.-P. Chaboureau[2]

Received 5 February 2008; revised 7 April 2008; accepted 14 April 2008; published 9 August 2008.

[1] We present a novel climatology of upper-tropospheric troughs and associated precipitation in the Mediterranean region, using 6 years (2001–2006) of Advanced Microwave Sounding Unit data. Troughs are more frequent or persistent during November through March in the whole of the Mediterranean basin, with up to 25% of days in the northwestern part of the basin. The interannual variability of number of intrusions is stronger from September through June. During summer, the variability is reduced, except in the NW region, and no troughs were observed in the SE region. Moderate precipitation occurs in at least 60% of the cases when an upper-level trough is present with weak seasonal dependency. In the southern Mediterranean moderate precipitation is an ubiquitous feature and presents small year-to-year fluctuations. The occurrence of deep convective rain associated with trough is lower, around 50%, and reduces to 20% in the northern part of the basin during winter. This occurrence varies a lot with individual years, especially in the southern Mediterranean. Upper-level troughs have more often a N–S orientation but, while no particular dependency of frequency of precipitation (whether moderate or convective) on their inclination was found, the location of precipitation is generally favored downstream. The North Atlantic Oscillation and Scandinavia patterns were found to be the most important large-scale circulation modes influencing the variability of number of intrusions, but the East Atlantic/West Russia and East Atlantic patterns are also important in the southeast region.

Citation: Funatsu, B. M., C. Claud, and J.-P. Chaboureau (2008), A 6-year AMSU-based climatology of upper-level troughs and associated precipitation distribution in the Mediterranean region, *J. Geophys. Res.*, *113*, D15120, doi:10.1029/2008JD009918.

1. Introduction

[2] High impact weather phenomena are rather frequent in the Mediterranean region. Its geographical location, with latitudinal range from the subtropics to midlatitudes, the complex orography surrounding the Mediterranean sea, and the large supply of water vapor at low levels, are all factors that contribute to severe weather conditions. The large population density in the Mediterranean makes this region particularly vulnerable to such events which cause severe social and economical distress. In addition, the Mediterranean has been identified as one of the most responsive to global climatic change [e.g., *Hulme et al.*, 1999; *Giorgi*, 2006]. For all these reasons, it is important to understand the climatological picture of these severe weather conditions. Severe weather encompasses conditions such as heavy precipitation and floods, strong winds and droughts. In our study we focus on heavy precipitation, and more specifically, we concentrate on the climatological study of upper-level troughs that intrude into and affect the Mediterranean region as well as on the occurrence of moderate to heavy precipitation in association with such intrusions.

[3] *Jansà et al.* [2001] showed that in the period of 1992–1996 in the western Mediterranean, 90% of the more than 900 cases of heavy rain occurred in association with a cyclone, regardless of its intensity. Other studies have demonstrated that precipitation in the cold season in the eastern Mediterranean are often associated with cyclones or surface lows [*Kahana et al.*, 2002; *Zangvil et al.*, 2003; *Tvieli and Zangvil*, 2007], but the origin and trajectories of air are also of importance in determining the location and intensity of rainfall over Israel [*Zangvil and Druian*, 1990; *Krichak et al.*, 2004]. There are however events of extreme precipitation in which no surface cyclone in the vicinity has been observed [*Jansà et al.*, 2001; *Turato et al.*, 2004] and local forcing allied to orography was enough to ensue favorable conditions for heavy rainfall. Other authors have related the occurrence of heavy precipitation to upper-level trough-like structures [e.g., *Massacand et al.*, 1998; *Fourrié et al.*, 2003; *Kotroni et al.*, 2006], and mesoscale convective systems [e.g., *Riosalido*, 1990; *Delrieu et al.*, 2005; *Ducrocq et al.*, 2003, 2004]. Very often interaction of upper-level systems (such as troughs, cyclones, jet streaks and tropopause folds) and surface depressions leads to specific configurations that are favorable to strong rainfall. The

[1] Laboratoire de Meteorologie Dynamique (IPSL/CNRS), Ecole Polytechnique, Palaiseau, France.
[2] Laboratoire d'Aérologie, UPS/CNRS, Toulouse, France.

0148-0227/08/2008JD009918

occurrence of heavy precipitation is therefore a multiscale phenomena, and is dependent not only on the presence of atmospheric depressions, but also on the topographic features and on moisture availability and distribution. For example, *Nuissier et al.* [2008] and *Ducrocq et al.* [2008] have demonstrated that a slow evolving synoptic environment, allied to orographic forcing, convergence of air at low levels, and strong evaporation played key roles on the persistence and intensity in three events of heavy precipitation in south of France.

[4] Regions where occurrence of heavy precipitation is frequently observed include the Gard region in France, the Balearic Islands and south of Spain, and the mountainous coast along the northern edge in eastern Mediterranean (e.g., *Nuissier et al.*, 2008, and the Mediterranean Experiment (MEDEX) database, http:/medex.inm.uib.es/). In these regions, heavy precipitation often occurs downstream of upper level cyclones or troughs when the induced flow pounds moisture-rich air on orographic barriers surrounding the Mediterranean Sea, forcing the ascent of unstable air masses and promoting the release of conditional instability [*Doswell et al.*, 1998; *Massacand et al.*, 1998; *Lionello et al.*, 2006]. The southside of the Alps is another region where heavy precipitation events have been historically frequent, and is a region vulnerable to flash floods due to its specific topography with several small river catchments [*Frei et al.*, 2001; *Jasper and Kaufmann*, 2003; *Walser and Schär*, 2004]. Heavy precipitation in this area was found to be commonly associated with narrow, deep and elongated upper-tropospheric streamers that move eastward from western Europe [*Massacand et al.*, 1998; *Chaboureau and Claud*, 2006; *Hoinka et al.*, 2006; *Martius et al.*, 2006]. In particular, streamers that are nearly north–south oriented and reach southward between the Pyrenees and northern Africa are found to be precursors of storms in the Alpine region.

[5] There have been several climatological studies of cyclones and cyclonegenesis in the Mediterranean region aiming at characterizing the subareas and mechanisms of cyclogenesis and their monthly or seasonal variability, which relied mainly on reanalysis data sets and/or simulations [*Alpert et al.*, 1990a, 1990b; *Trigo et al.*, 1999, 2002]. *Chaboureau and Claud* [2006] presented an alternative climatology of Mediterranean cloud systems and upper level disturbances based on 8.5 years of TIROS Operational Vertical Sounder (TOVS) satellite data, in which cloud systems and upper level troughs were detected using a complex inversion technique [*Chaboureau et al.*, 2001; *Chaboureau and Claud*, 2003]. They showed that an upper level anomaly is found upstream in about 30% of the cloud systems in winter, 26% in spring and 7% in autumn (but 23% in October). They could not say however, what proportion of the cloud systems was associated with heavy precipitation mainly due to limitation of TOVS spatial resolution. Since the late 1990s TOVS has been replaced by the ATOVS (Advanced TOVS), which includes the Advanced Microwave Sounding Unit (AMSU) instrument with improved horizontal and spectral resolutions.

[6] In this study we provide a climatological description of upper level troughs (ULTs) and associated precipitation in the Mediterranean region, using AMSU data. This is a novel approach for two important reasons: First, this climatology relies mainly on direct AMSU observations; second, we examine the link between ULTs and precipitation, in contrast with and complementing the above studies which mainly examined the existence and characteristics of ULTs in the presence of clouds and/or rain. *Funatsu et al.* [2007] have demonstrated the potential of AMSU to detect ULTs that are associated with severe storms in the Mediterranean basin, as well as precipitating and convective areas. The use of satellite observations is attractive because it provides a homogeneous data set, covering the whole of the Mediterranean region including over the sea, where in situ measurements are scarce. In addition, AMSU provides the possibility of analyzing the concomitant evolution of the upper level system and the development of precipitation. We investigate what is the frequency of ULTs in the Mediterranean, and which proportion of those yield significant precipitation. We also examine whether the shape of the ULTs influence the frequency and/or intensity of precipitation, as well as the relative position of precipitation areas with respect to the ULT. Finally, we examine the signal of large-scale circulation patterns that are mostly significant in the Mediterranean on the number of intrusions and precipitation.

[7] The structure of the paper is as follow: Section 2 describes AMSU data, while in section 3 we describe the rationale and procedure for defining an objective searching criteria of ULTs. The climatology of ULTs and associated precipitation based on the proposed criteria is presented in section 4.1, while in section 4.2 we discuss their interannual variability. In section 4.3 we address the dependency of the frequency of precipitation and convection on the shape of the ULT, and its relative position of occurrence. The modulation of intrusion events and precipitation by the large-scale atmospheric circulation is discussed in section 5. Finally, Section 6 presents a summary of the results and final remarks.

2. Data

[8] AMSU is a cross-scanning microwave instrument which consists of two modules: AMSU-A which has channels in the molecular Oxygen frequencies (50–58 GHz), mainly designed for atmospheric temperature profile retrieval, and AMSU-B which has three channels centered at 183 GHz (water vapor absorption line), designed for optimal moisture retrieval. Furthermore, both modules have window channels, which are not used in this study. The swath width of both AMSU-A and AMSU-B is of approximately 2300 km; the near-nadir instantaneous field of view of AMSU-A is 48 km while AMSU-B has a near-nadir resolution of 16 km.

[9] AMSU has been collecting data onboard NOAA polar-orbiting satellites starting in 1998. In the present study we use NOAA-16 (launched on 21 September 2000) AMSU-A and -B for the period of January 2001 to December 2006, as it consists of an homogeneous data set and avoids intersatellite biases. NOAA-16 AMSU-B has small scan asymmetries, comparable to the instrument noise [*Buehler et al.*, 2005] while AMSU-A data presents scan asymmetries, but the effect is mostly significant in the window channels (23.8, 31.4, 50.3 and 89 GHz); for the remaining AMSU-A channels this effect is attenuated by the presence of the atmosphere [*Weng et al.*, 2003]. Further details on the instrument can be found in the NOAA's KLM

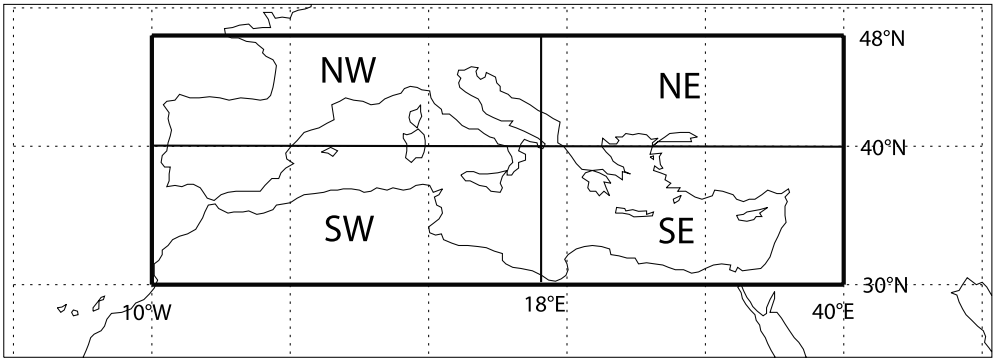

Figure 1. Mediterranean domain and subdomains considered in this study: NW [40–48°N, 10°W–18°E], SW [30–40°N, 10°W–18°E], NE [40–48°N, 18–40°E], SE [30–40°N, 18–40°E].

User's Guide available online at http://www2.ncdc.noaa.gov/docs/klm/.

[10] We use AMSU-A channel 8 for detection of ULTs, as further explained in Section 3. AMSU-B moisture channels (3 to 5) detect the presence of hydrometeors through the scattering of radiation which lowers the brightness temperature compared with its surroundings [e.g., *Greenwald and Christopher*, 2002]. AMSU-B channel 3 minus 5 (hereafter B3m5) is used for detection of moderate precipitation: An increase in B3m5 indicates a large scattering effect by hydrometeors in the low troposphere. A threshold of B3m5 ≥ -8 K was found to correspond statistically to a rainfall of at least 10 mm in 3 hrs when compared with the Tropical Rainfall Measuring Mission (TRMM) 3B42 three hourly accumulated precipitation product, as well as with radar and rain gauges from meteorological ground stations [*Funatsu et al.*, 2007]. The deep convective threshold (DCT), used to detect convective areas, was initially proposed to identify convection in the tropical regions [*Hong et al.*, 2005]. It is defined through the criterion that B3m5, B4m5 and B3m4 (i.e., AMSU-B channels 4 minus 5, and 3 minus 4, respectively) are simultaneously greater or equal 0, and comparison with TRMM showed that DCT corresponds to an accumulated rainfall of at least 20 mm in 3 hrs in 50% of the cases. Both thresholds were validated for rain detection in the Mediterranean over surfaces free of snow and ice [*Funatsu et al.*, 2007]. Over snow-covered areas or very cold surfaces (for example mountainous regions during winter) these thresholds per se cannot discriminate between frozen hydrometeors and a cold surface under clear sky. Therefore we used the additional constraint that a precipitating region must attain a upper tropospheric humidity (UTH) relative to ice of at least 70%. This UTH was calculated using the formulation proposed by *Buehler and John* [2005] using channel 3 of AMSU-B. We stress that we use AMSU-B for detection of precipitation only, and we do not try to quantify rain rates or exact accumulated precipitation. In the remaining of the text, "precipitation" refers to rainfall detected using the criterion B3m5 ≥ -8 K, while "convection" and "convective areas" are specifically used to denote areas satisfying the DCT criterion, with heavy precipitation.

[11] AMSU-A data was corrected for limb effect using coefficients derived by from the Radiative Transfer for TOVS (RTTOV). Details on the correction procedure can be found in *Funatsu et al.* [2007]. After the limb correction, the data was resampled to a regular $1° \times 1°$ lat/lon grid, using a smoothing criteria of $1 - (r/rd)^2$, where r is the distance of the actual data point to the fixed grid point, and rd is the radius of search arbitrarily fixed to 2.5. For AMSU-B the brightness temperature (BT) data was resampled without smoothing to a regular grid of $0.2° \times 0.2°$, using a weighting of $1/r^2$, where r is again the distance of the actual data point to the fixed grid point. Consecutive satellite passes covering the domain of 10–60°N 10°W–50°E were concatenated in their descending and ascending (approximately between 22-03 UTC and 08-12UTC, respectively) motions providing a twice daily BT information for this area. The target area used in this study (the Mediterranean region) is effectively the area comprised between 30–48°N 10°W–40°E, and we considered further subdomains to examine regional differences (Figure 1): NW [40–48°N, 10°W–18°E], SW [30–40°N, 10°W–18°E], NE [40–48°N, 18–40°E], SE [30–40°N, 18–40°E].

3. Detection of Potential Vorticity (PV) Intrusions Using AMSU-A Channel 8

[12] An objective method for detection of upper-level systems that may be precursors of strong storms using AMSU data only was devised. Channels 7 and 8 of AMSU-A have weighting functions peaking at around 300 and 200 hPa, respectively, which makes them good candidates for ULT detection. However, because channel 7 has also considerable contribution from the lower troposphere, we investigated the performance of channels 7 minus 5 instead of channel 7 by itself, in an attempt to reduce this effect. Detailed analysis of 6 case studies of severe storms between September and December (i.e., covering fall and winter seasons) showed that these events were associated with stratospheric intrusions with very large PV ($\gg$4 PVU). Vertical cross-sections through such intrusions showed a corresponding PV anomaly of at least 1 K concentrated around 250 hPa, thus "creating" a warm brightness temperature signal detected by the upper-tropospheric channels of AMSU-A [*Funatsu et al.*, 2007]. Channel 8 (hereafter, A8), was able to detect such structures compared with maps of potential vorticity (PV) at 250hPa, and performed better than the difference of channels 7 and 5 to detect such PV anomalies. Furthermore, values of A8 larger than 221 K were found to be nearly coincident with areas of large PV at 250 hPa suggesting that this value could be used as a

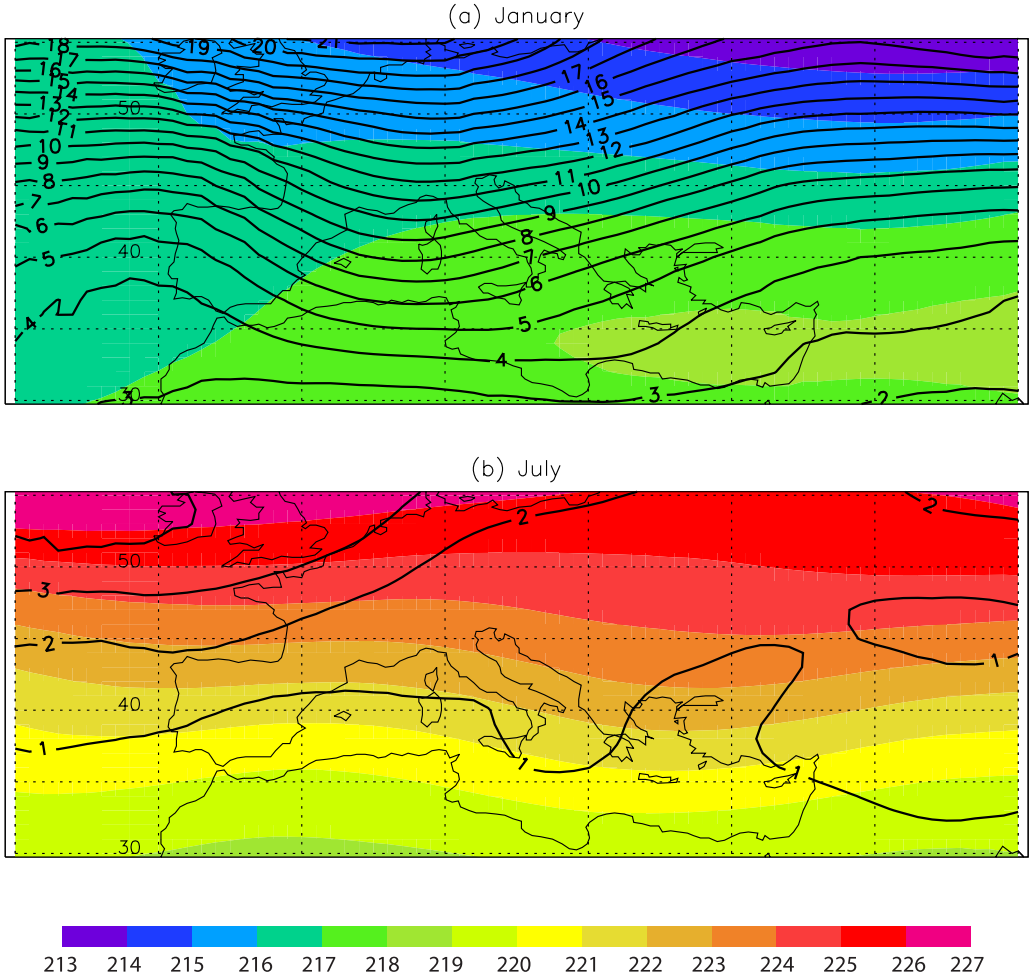

Figure 2. Average AMSU-A channel 8 (A8) brightness temperature (BT) (color) and variance (solid contours), in K, for January (a) and July (b), relative to 2001–2006.

threshold for ULT detection. However, *Funatsu et al.* [2007] also observed that for a case of very intense PV intrusion and heavy precipitation in southern France in September 2002, the value of 221 K was too low to isolate the intrusion (see their Figure 7e), and concluded that further analysis was necessary to find thresholds for ULT detection.

[13] A difficult aspect of determining thresholds to objectively detect ULTs using A8 BT regards its validity for all seasons or even months. To illustrate this point, consider Figures 2a and 2b which shows the average A8 BT and its variance for January and July, respectively, for the period 2001–2006. In January, the average A8 BT in the Mediterranean basin ranges between 216–219 K and there is large latitudinal gradient in the variance. In July, A8 BTs range from 220 to 224 K, and BT increases northward. The variance in July is small, with weak gradient, in the order of 2 K. The seasonal fluctuation and reversal in the BT gradient would create unwanted degrees of arbitrariness for objective detection of ULTs based solely on this parameter. To mitigate the subjectiveness of the criteria, we sought for an alternative identifier based on A8 BT anomalies (BT′) relative to a mean monthly value calculated over the period 2001–2006. Another possibility, not explored here, would be to use a normalized BT′ with respect to a local or regional standard deviation. In general, we expect A8 BT′ to have a seasonal fluctuation with smaller amplitude than of A8 BT itself.

[14] In a first step, we searched for a value of A8 BT′ that would be representative of a strong upper level intrusion, as those found in the vicinity of heavy precipitating areas. Such BT′ was estimated by examining case studies of intense rainfall both in winter and summer, in which upper-level PV "troughs" were present. Three examples comparing PV at 250 hPa and BT′ for the cold and summer seasons are shown respectively in Figures 3 and 4. Based on these case studies (and others not shown), we found that a representative value for a strong intrusion (i.e., with PV at 250 hPa $\gg$ 4 PVU) is BT′ > 2 K. Exception is noted for the case of August 2002, for which BT′ is of only $\sim$1 degree coincident with PV values well above 4 PVU. Similarly, troughs with maximum PV at 250 hPa of the order $\sim$4PVU also do not show a corresponding BT′ field, e.g., a system over Turkey on 10 November 2001 (Figure 3a), and over south Italy on 31 July 2002 (Figure 4a). This indicates that weak PV anomalies do not show a BT′ counterpart and will not be detected by a threshold of BT′ > 2 degrees.

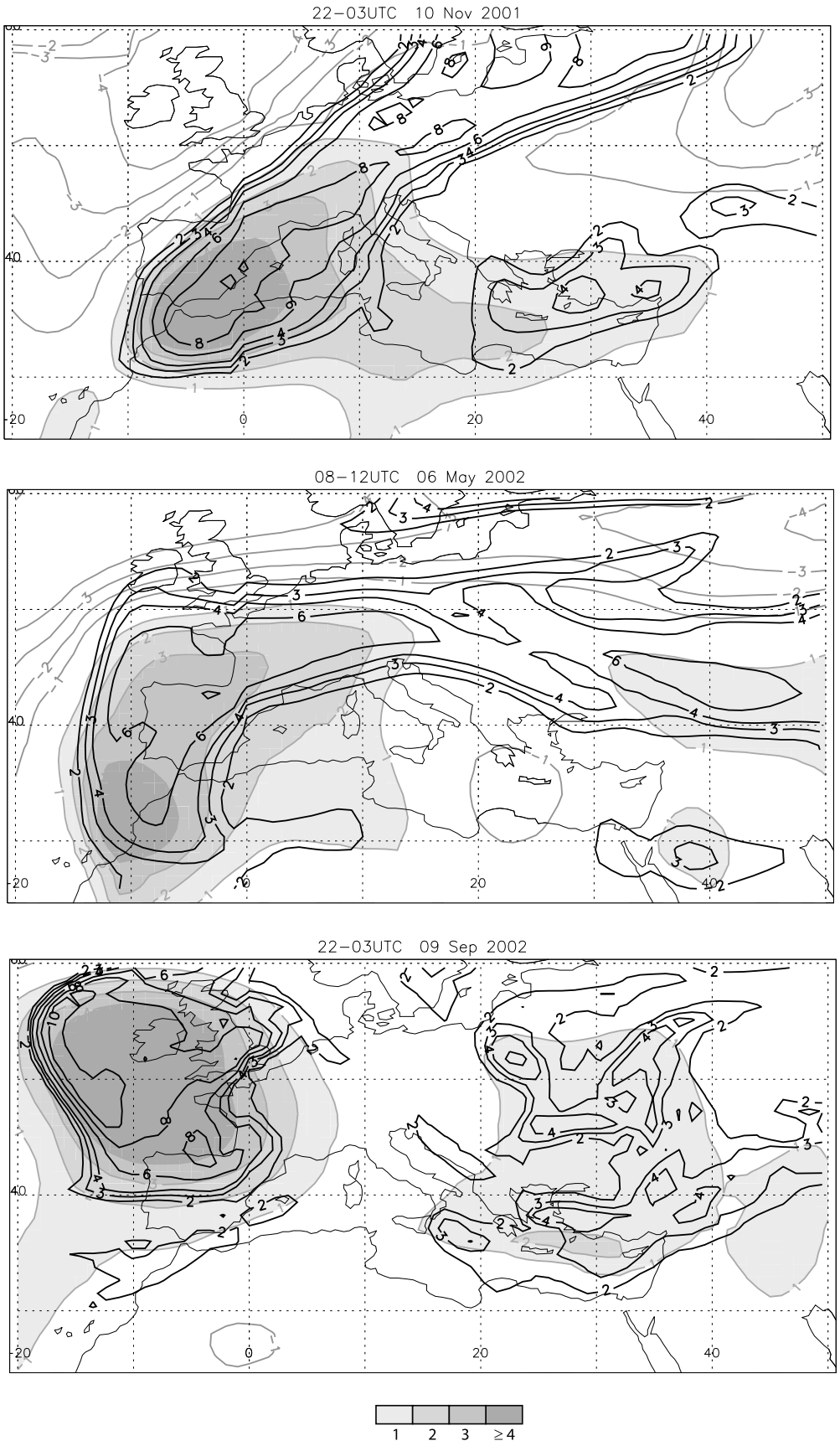

Figure 3. Winter and transition months cases: A8 BT anomaly (BT′, in K) relative to a monthly mean of 2001–2006 (shaded > 1 K, gray contours < −1 K) and PV at 250 hPa (PVU, 1 PVU = 10^{-6} K m^2 kg^{-1} s^{-1}; black contours) for the dates indicated on the top of each panel.

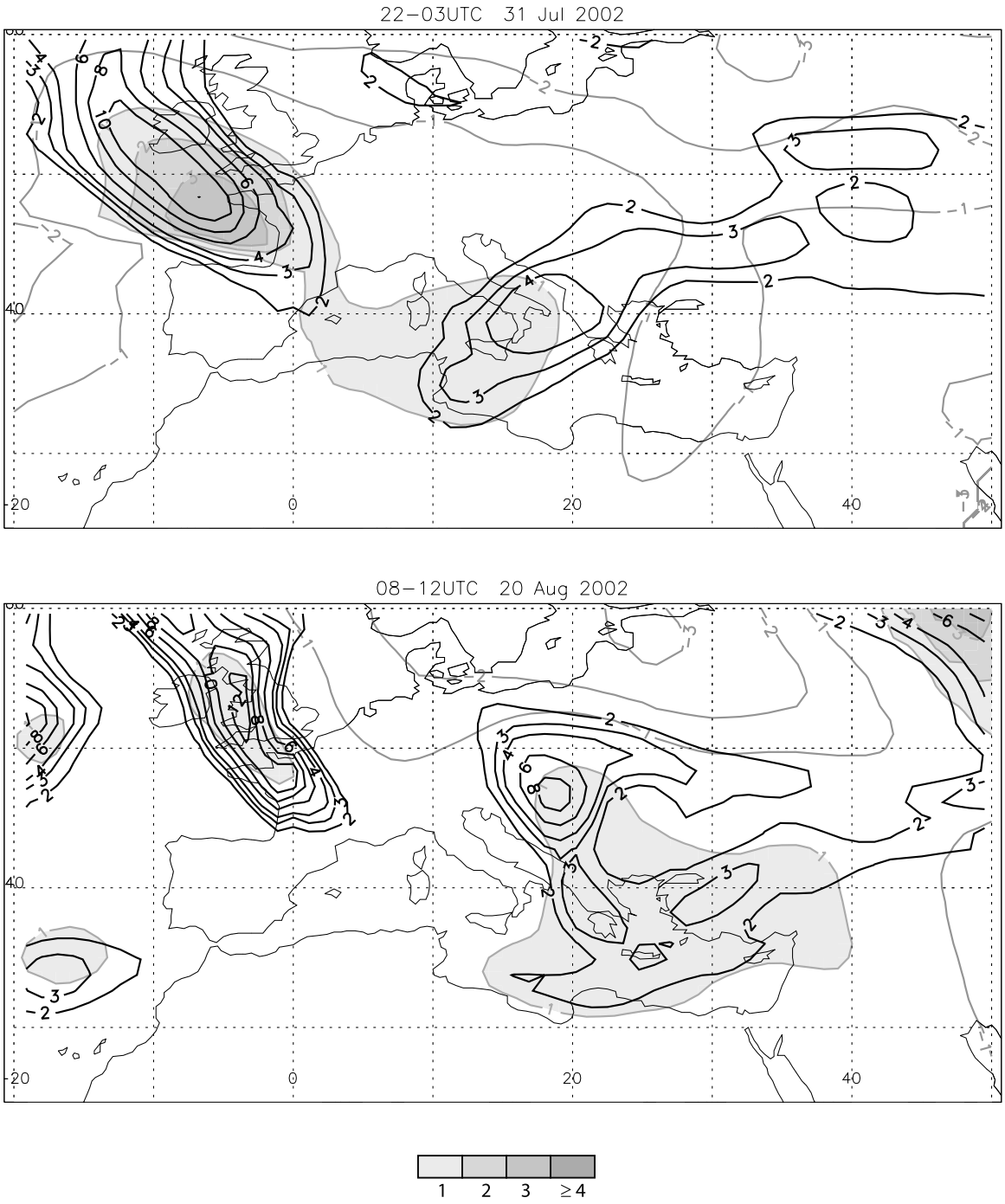

Figure 4. Summer cases: A8 BT′ (K) relative to a monthly mean of 2001–2006 (shaded > 1 K, gray contours < −1 K) and PV at 250 hPa (PVU; black contours) for the dates indicated on the top of each panel.

[15] We then investigated the seasonal fluctuation of A8 BT′ in the Mediterranean region: Figure 5 shows the monthly variation of the maximum BT′ $\geq$ 2 K for each year (colors), as well as the average of all years (black). The values are area-weighted, i.e., normalized according to the area that each system covers (to the nearest lower integer value) relative to the entire search domain. In this manner, anomalies with small area coverage are given less weight. This figure show that systems have on average maximum BT′ amplitudes between 3–5 K, and are stronger in the cold months than in the summer. The seasonal fluctuation arises as a response to the vertical displacement of the tropopause: during winter the tropopause is lowest and A8 probes the tropopause and lower stratosphere, while during summer it is high and A8 samples the upper troposphere. This means that ULTs occurring during summer are located higher up in the atmosphere and only very strong and vertically deep ones will be detected by A8.

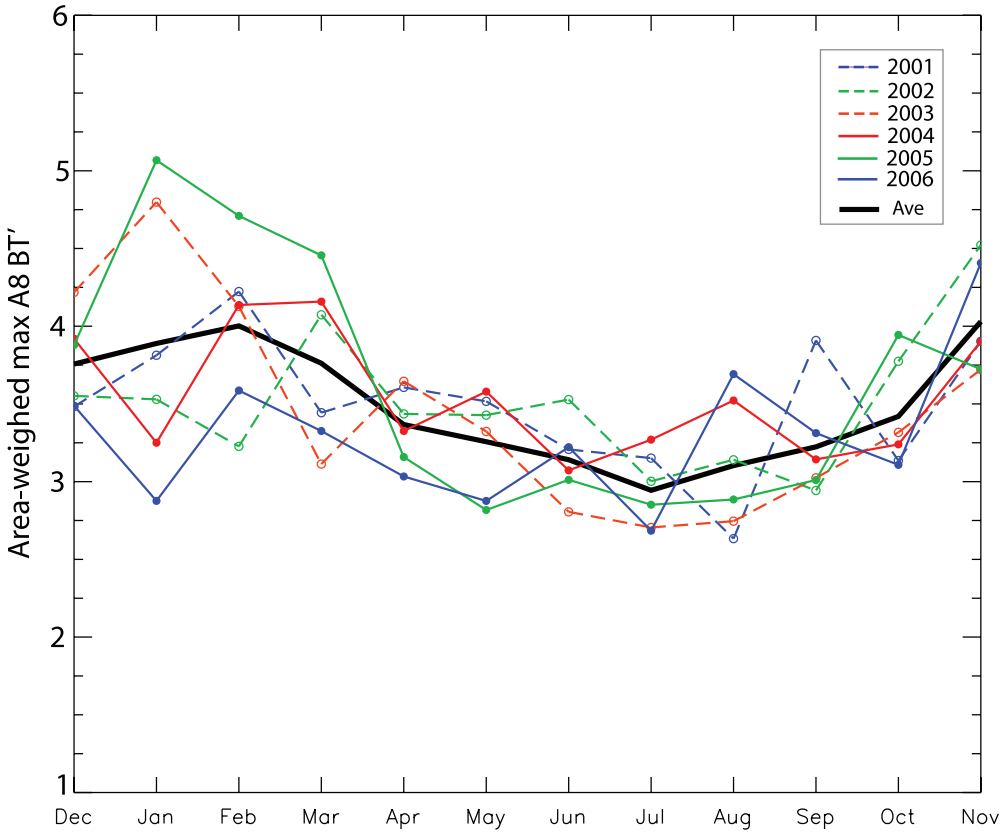

Figure 5. Monthly variation of the maximum BT′ (K) found for each event in which BT′ > 2 K for 2001–2006 (dashed) and average of these years (thick solid). The maximum BT′ is normalized by the area that the system covers (to the nearest lower integer value) relative to the entire search domain; see text for details.

[16] For the purpose of objectively detecting ULTs, a value of BT′ $\geq$ 3 K was chosen because this threshold is representative of strong ULTs during fall and winter seasons, and it is in these seasons the strongest storms in the Mediterranean basin have been registered (e.g., MEDEX). The sensitivity of the results presented here to the threshold value was found to be small, and will be further discussed in section 6. The identification of an ULT is made through an objective procedure that, for each day, searches the maximum A8 BT′ in the domain; if the maximum falls into the criterion (A8 BT′ $\geq$ 3 K) it is identified as the center of the ULT. The processing code can identify up to 3 centers at a given time, as long as they are not embedded in a common isotherm of BT′ $\geq$ 3 K. Once these centers are found, we identify the subdomain to which they belong.

4. Climatology

4.1. Upper-Level Troughs and Associated Precipitation

[17] Using the above described procedure, we formed a climatology of ULTs based on A8 data. Figure 6a shows the monthly average number of days with ULTs (A8 BT′ $\geq$ 3 K) for each quadrant. Notice that since we do not use a tracking procedure, one evolving ULT is counted more than once as long as it holds the A8 BT′ threshold. For all subdomains events reaching the proposed criterion of strong ULT are more abundant or persistent during November to March, with decreasing frequency from March through July. The number of events is nearly twice as much in the western than in the eastern Mediterranean regions from December to May, while for the period of June through October, upper level systems reaching the proposed criterion are mostly confined in the NW quadrant. Overall, there are more ULTs in the NW and less in the SE, throughout the year. Moreover, there are no ULTs during August and September in the SE region. The average equivalent radius (i.e., the radius that the system would have if the grid points for which the criterion is reached would fill up a circular area) also varies along the year (Figure 6b), with systems with equivalent radius between 500–400 km typical of winter and spring. Systems reaching A8 BT′ $\geq$ 3 K are much smaller during summer in the SW, NE and SE regions, while they remain larger and nearly unchanged in the NW region. The above results are in agreement with the stratosphere–troposphere exchanges climatology by *Sprenger and Wernli* [2003] who showed that stratosphere-to-troposphere transfers are frequent over the Mediterranean during spring, while *Sprenger et al.* [2007] showed that these exchanges are usually related to a PV structure (60 to 80% of the cases).

[18] Figures 6c and 6d show the relative frequency of occurrence of rain and convective areas within a range of 10 degrees north, west and south and 15 degrees to the east of the center of maximum anomaly; that is, every time that a grid point with B3m5 ≥ -8 K is found, the event is counted

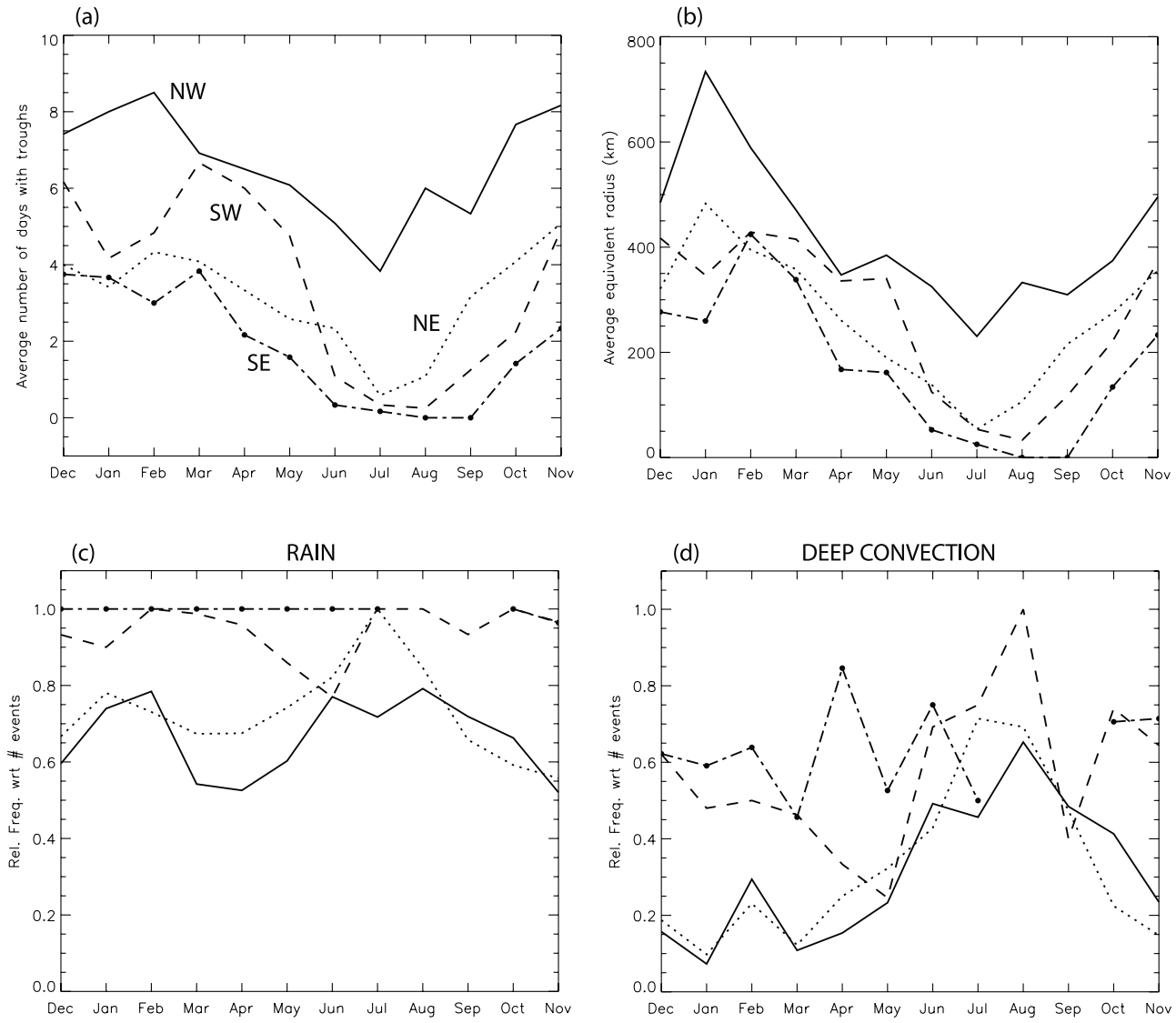

Figure 6. (a) Average number of events in which A8 $BT' \geq 3$ K was detected, for the period 2001–2006, as a function of month. (b) Average equivalent radius of the events (km). Relative number of events in which A8 $BT' \geq 3$ K was detected and accompanied with rain (c) or convection (d). NW, solid; NE, dotted; SW, dashed; SE, dash-dotted.

as positive for occurrence of rain (and similarly, when DCT is satisfied, the event is counted as convective). The area of search is slightly larger to the east as the occurrence of precipitation is expected to be downstream of ULTs, as a consequence of quasigeostrophic dynamics [e.g., *Holton*, 1992; *Dutton*, 1995]. Figure 6c shows that in the cold months the northern half of the basin has a relatively low frequency of rainy events associated with ULTs (50–75%) compared to the southern half (75–100%). There is very weak seasonal dependency of this frequency for all domains, except SE, where there are no events in the summer (and therefore no associated precipitation). The result for the SE region is comparable with the results of *Ziv et al.* [2006] who found that ULTs extending from eastern Europe toward the eastern Mediterranean and rainfall between December and February have a very close link, expressed by a correlation of −0.74.

[19] The relative frequency of convective events (Figure 6d) shows a strong seasonal dependency, with low values in the northern half of the basin (10–30%) compared to the southern part (around 60%) from December through April, and a sharp increase in the relative frequency from May through August in all regions except SE. When these results are analyzed in conjunction with Figure 6a we see that although the number of ULTs decreases toward the summer, the frequency of such events that are accompanied by rain and convection increases. However, given that cloud systems are frequent throughout the year with weak seasonality [*Chaboureau and Claud*, 2006], these results imply that local thermodynamical and/or orographic conditions are of primary importance to explain precipitation in summer. This is particularly true for the SE region [e.g., *Saaroni and Ziv*, 2000].

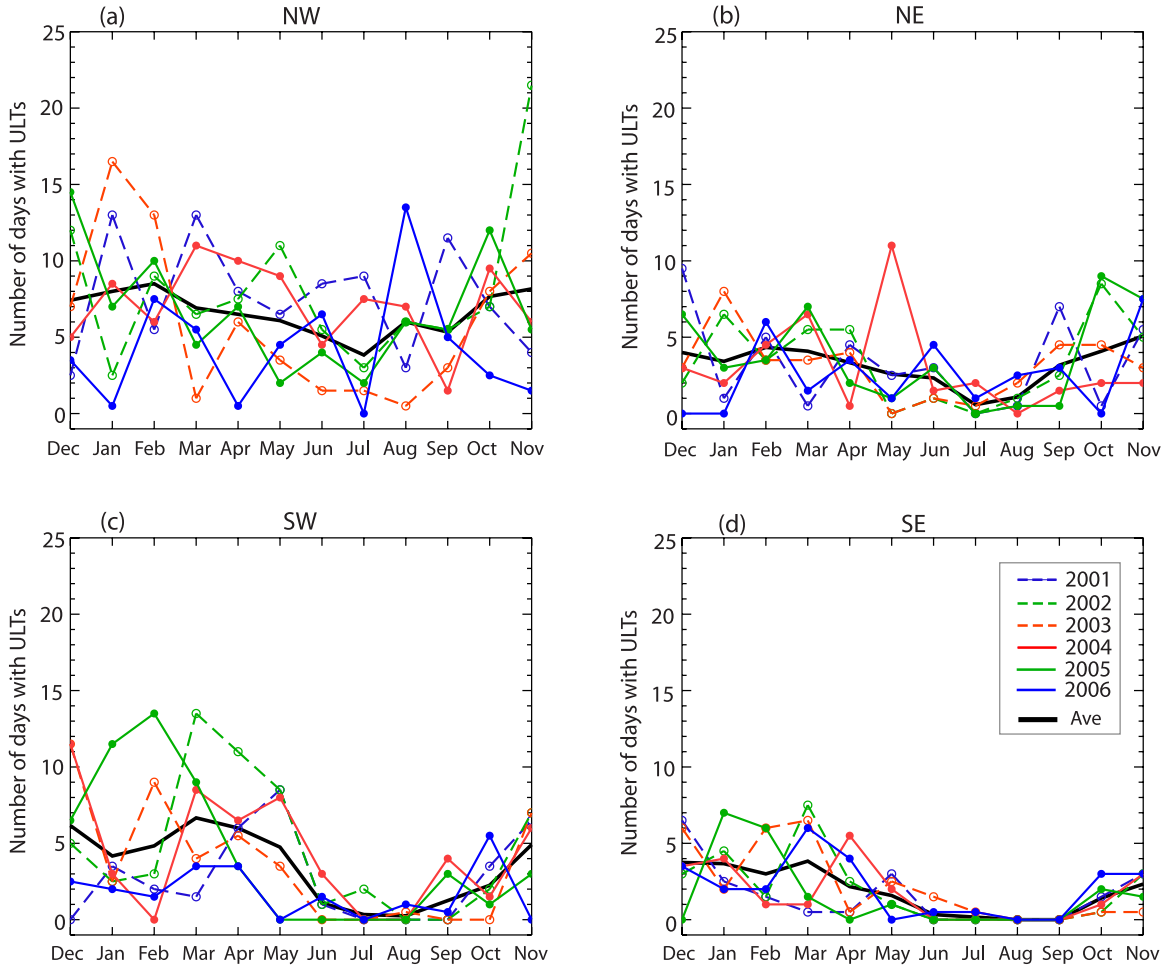

Figure 7. Interannual variation of number of events in which A8 $BT' \geq 3$ K was detected for regions NW (a), NE (b), SW (c), and SE (d). Average of 2001–2006 is shown in bold black, and individual years are shown in color.

[20] As for the inverse relationship (i.e., the presence of an ULT whenever there is heavy precipitation) *Martius et al.* [2006] based on ERA-40 data showed that in 73% of the days with extreme precipitation along the Swiss Alpine south side (defined as having at least 29 mm accumulated in 24 hr) there was an upper level streamer upstream, and during autumn, this percentage was as high as 85%. However, in winter the percentage was of only 30%. Our climatology show that for the NW region, the percentage of heavy precipitation associated with ULTs is of 50 to 25% from September through November, with decreasing efficiency toward the cold months. These differences in frequency arise naturally since we are not considering only the Alpine region, but a much larger domain which contains miscellaneous environments which allows the frequency of precipitation to be diluted compared with targeting a specific location.

4.2. Interannual Variability of ULTs and Frequency of Associated Precipitation

[21] The results obtained in the preceding section refer to the average frequency association between ULTs and precipitation and convection, however it does not say how robust is this association. Here we address this issue by exploring the year-to-year fluctuations around the average. The interannual variability of the ULT for each subdomain is shown in Figure 7, while the average and standard deviation (rounded to the nearest integer) is shown in Table 1a. There is large variability of the number of events for all regions in the winter and spring. Only NW region presents large variability throughout the entire year including summer, while for the other regions the variability in summer is very reduced and presents very few events for all years. The large variability, in particular in the NW region, is partly explained by the influence of large scale circulations over the Atlantic and over northern and central Europe [e.g., *Eshel and Farrell*, 2000; *Chaboureau and Claud*, 2006; *Yiou et al.*, 2007]. This issue will be addressed in more details in the next section. Another important source for the large variability stems from the fact that we use a rather short period (6 years) which emphasizes the effect of fluctuations on the frequency of ULTs crossing the Mediterranean region.

[22] It is interesting to note that in 2003 there was a local minimum in the number of ULTs from June to August in the NW region, coinciding with the dry and hot spell that western Europe experienced in that year [e.g., *Vautard et al.*, 2007; *Fischer et al.*, 2007]. *Vautard et al.* [2007]

Table 1. Average ($\bar{n}$) and Standard Deviation (s)[a]

	NW		NE		SW		SE	
Month	$\bar{n}$	s	$\bar{n}$	s	$\bar{n}$	s	$\bar{n}$	s
(a) Number of Days With ULTs								
January	8	6	3	3	4	3	4	2
February	9	3	4	1	5	5	3	2
March	7	4	4	2	7	4	4	3
April	7	3	3	2	6	3	2	2
May	6	3	3	4	5	4	2	1
June	5	2	2	1	1	1	0	1
July	4	3	1	1	0	1	0	0
August	6	4	1	1	0	0	–	–
September	5	3	3	2	1	2	–	–
October	8	3	4	4	2	2	1	1
November	8	7	5	2	5	3	2	1
December	7	4	4	3	6	4	4	2
(b) Frequency (%) of Precipitation								
January	74	14	78	15	94	23	100	0
February	80	21	73	22	100	0	100	0
March	55	20	67	32	99	2	100	0
April	53	25	68	36	96	4	100	0
May	63	21	74	19	86	9	100	0
June	77	15	82	19	77	23	100	0
July	72	13	100	0	100	0	100	0
August	81	36	85	20	100	0	–	–
September	81	13	66	29	93	8	–	–
October	70	21	59	28	100	0	100	0
November	54	21	56	24	97	6	96	6
December	62	14	67	13	93	7	100	0
(c) Frequency (%) of Convection								
January	8	38	10	7	48	20	59	23
February	30	20	23	26	50	25	64	29
March	11	9	12	10	47	9	44	29
April	15	12	25	16	33	14	85	16
May	25	15	32	13	25	6	53	14
June	49	22	43	21	69	39	75	56
July	46	10	71	26	75	0	50	50
August	69	32	69	37	100	0	-	-
September	55	12	47	25	40	35	-	-
October	43	26	22	37	74	35	71	38
November	24	17	15	10	64	18	71	25
December	16	11	19	15	65	19	62	12

[a](a) Number of days with ULTs with BT′ $\geq$ 3 K (values rounded to the nearest integer), (b) frequency (%) of precipitation associated with ULTs, and (c) frequency (%) of convective precipitation associated with ULTs, for the period 2001–2006, for each of the subregions shown in Figure 1.

showed that the dry summer in Western Europe was related to the hydric deficit in southern Europe in the previous seasons. Our analysis shows that the number of ULTs in early 2003 was below the average in March and from May onward, therefore the absolute frequency of precipitation associated with these ULTs was also reduced, in agreement with the study of *Vautard et al.* [2007]. Another minimum is observed in July 2006 for the NW, coinciding with a dry spell period in the region (although ample news coverage and press reports from Meteorological agencies were released, scientific documentation is available only for the 2003 (European) heatwave. For 2006 heatwave press releases, see e.g., http://www.bbc.co.uk/weather/world/news/19072006news.shtml, http://www.dw-world.de/dw/article/0,2144,2116999, 00.html, http://www.metoffice.gov.uk/corporate/pressoffice/2006/pr20060904a.html, http://www.eorc.nasda.go.jp/en/imgdata/topics/2006/tp060922.html). In this year, no strong ULT was detected in the NW region (western Europe). Furthermore, from September through December 2006 there were fewer than average ULTs in this region, and this also coincides with an exceptional warm autumn/winter of 2006 [*Luterbacher et al.*, 2007; *Yiou et al.*, 2007].

[23] Figures 8 and 9 show the related interannual variability of frequency of rain and convection associated with ULTs, respectively, while their average and standard deviation are shown in Table 1b and 1c. There is large interannual variability of frequency of rain for the northern part of the domain, in both western and eastern Mediterranean (Figures 8a and 8b). In the southern part the interannual variability is much smaller, with high frequency of moderate rain (Figures 8c and 8d). The low interannual variability suggests that the connection between ULTs and occurrence of moderate rain in the southern part of the Mediterranean is robust, supporting previous studies that have shown that precipitation in the Levant (SE Mediterranean) is mainly a winter feature, and is influenced by upper level systems passing through the region [e.g., *Saaroni and Ziv*, 2000; *Tsvieli and Zangvil*, 2007].

[24] The relative frequency of convection associated with an ULT for individual years is, however, much more spread around the mean (Figure 9 and Table 1c). Convective events between October and May have a more or less consistent frequency around the mean in the northern Mediterranean (Figures 9a and 9b), while in the southern half there is a large spread throughout the year (Figures 9c and 9d). This spread stems also from the relatively small number of cases. The large interannual variability of the frequency of convection associated with ULTs implies that their connection is weaker compared to intrusions and moderate precipitation. In all subdomains except SE, the frequency of convective events is higher between July and October. At the end of the summer and in autumn, the Mediterranean sea is warmest and the air has high water vapor content. As cold air masses incursion into the Mediterranean from the midlatitudes, they destabilize the atmosphere as they sweep over the warm waters, and conditions that are favorable to the occurrence of storms ensue.

4.3. ULT Axis of Orientation and Precipitation Distribution

[25] In the previous sections the frequency of rainfall and convection was analyzed in terms of their occurrence only. In certain locations, however, the orientation of the ULT has an impact on the location of the precipitation. One example is the Alpine southside in which a clear orientation of the axis of the ULT in the N–S direction is observed to the west of and preceding several heavy rainfall events [e.g., *Martius et al.*, 2006; *Chaboureau and Claud*, 2006]. Therefore in this section we investigate whether there is a general distinction of distribution of rainfall and convection depending on the ULT orientation.

[26] In a first step we defined objectively the inclination of the ULT axis. The objective method to determine the axis inclination was based on finding the direction, relative to the west–east direction cutting over the center of the trough, in which the gradient of A8 BT′ was weakest. As many ULTs have rather peculiar shapes, the results were somewhat sensitive to the area considered for calculation of such gradient. However, we found that the method is robust in the sense that it allows to identify coherent structures representing the ULTs, as shown further below. We consider

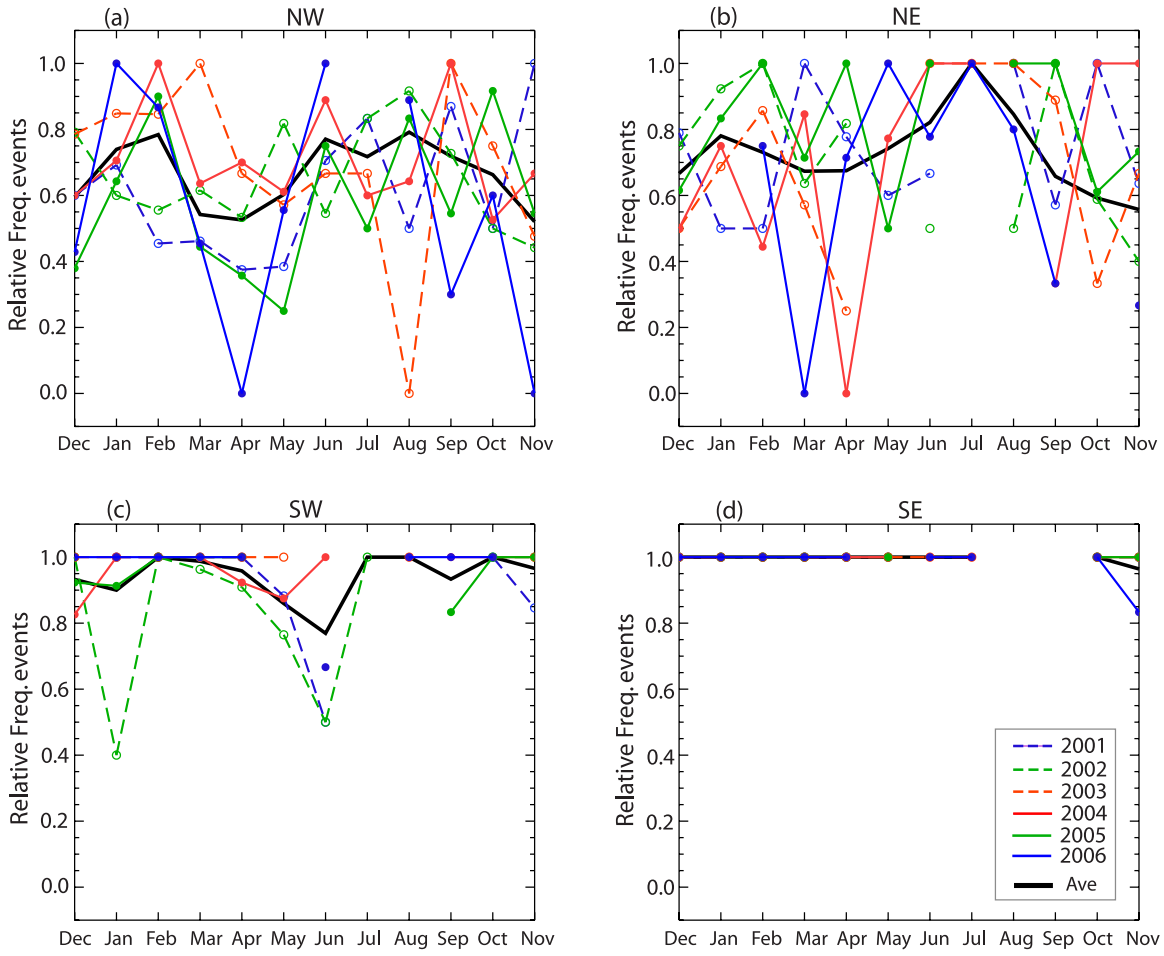

Figure 8. Interannual variation of number of precipitating events relative to the number of trough intrusions for regions NW (a), NE (b), SW (c), and SE (d). Same color key as in Figure 7.

4 axis inclinations, i.e., every 45°. A 0° inclination corresponds to A8 BT′ that is elongated in the W–E direction (with angles varying between −22.5° and 22.5°), while a 90° inclination corresponds to A8 BT′ elongated in the N–S direction (angles varying between 67.5° and 112.5°), and so forth (notice that the axis inclination is relative to geographical coordinates, and not to the mean flow). Then maps of precipitation distribution and frequency according to each inclination were examined.

[27] Figure 10 shows the average monthly frequency of ULTs with each angle of axis inclination for each subdomain. ULTs have more often inclination of around 90° in the northern Mediterranean and in particular in the NE (Figure 10b), with the other inclinations more or less equally distributed throughout the year. From November through May there is also a prevalence of troughs with inclinations of ∼90° in the SE (Figure 10d), however for the same period in the SW, troughs are oriented in ∼0° or ∼90° without a clear preference. The cause for a preference for inclinations of ∼90° in the eastern Mediterranean is not clear. One possible explanation is that as midlatitude (PV) wave breaks into the Mediterranean region, often the signal in the A8 BT′ is of a cut-off, "round" structure, slightly elongated in either the N–S or W–E direction (not shown). However, while there may be an impact of the life cycle of the upper level disturbance on the shape (orientation) of the trough, we cannot directly assess inclination changes with the evolution of the system based on our analysis because we do not have a tracking method.

[28] The seasonal composites of A8 BT′ for each ULT axis inclination and the cumulative absolute frequency of rain and convection occurrence are shown in Figures 11 and 12, respectively, for the entire Mediterranean region without further separation, for the sake of simplicity. The ULTs are colocated so that their center is at (0,0). These composites show that the A8 BT′ field presents coherent structures representing the ULTs. The composites of troughs with inclination of ∼90° for JJA and SON suggest that this category also includes rounder structures (with slightly weaker gradient in the N–S direction than in other directions), and could explain the relative high number of inclinations for this inclination. In terms of moderate rainfall, we observe that there is widespread precipitation from September through February independent on the axis of the trough, while in summer the precipitation is mostly concentrated "underneath" and to the east of the center of the ULT (Figure 11) mostly within a radius of 10. Convective areas are found more often and are larger downstream

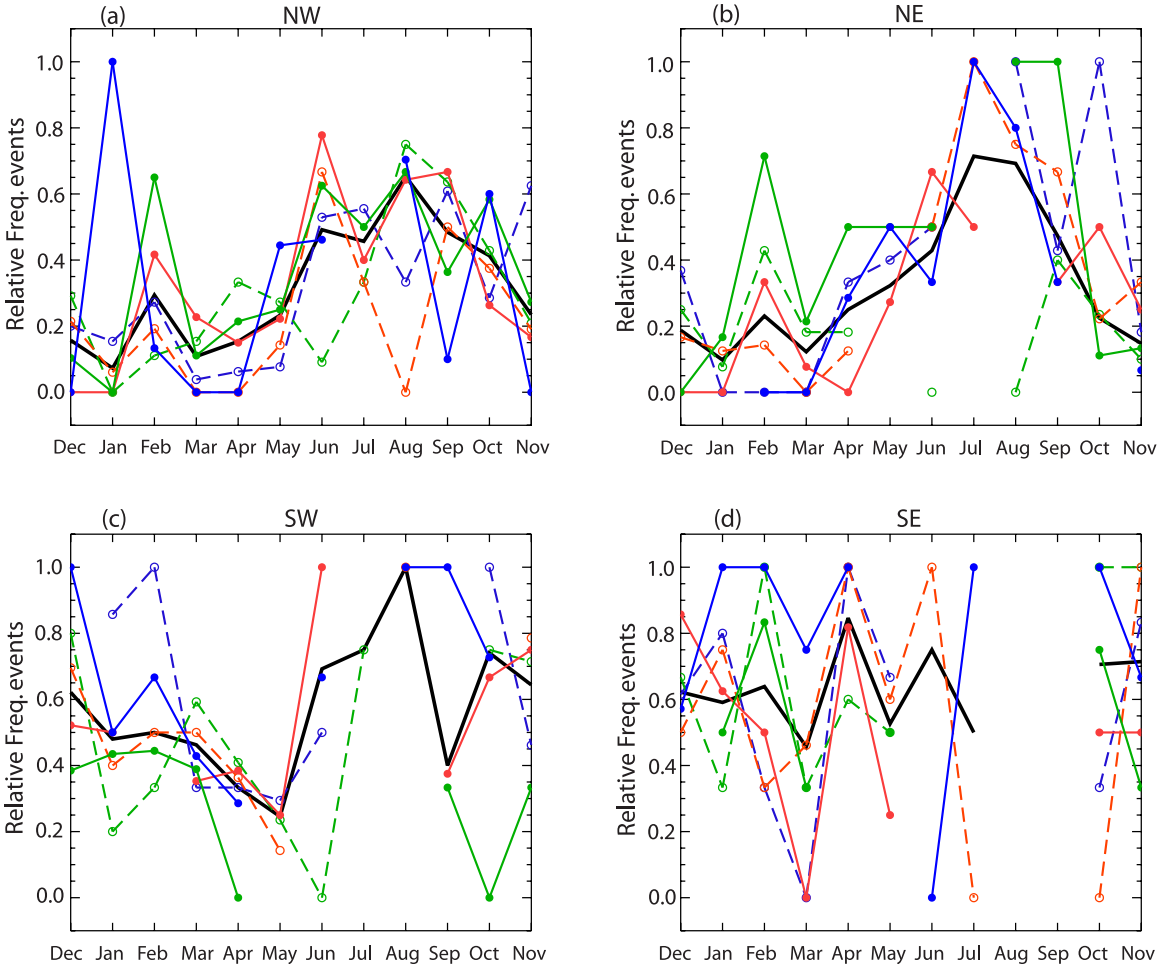

Figure 9. Same as in Figure 8, except for number of deep convective events relative to the number of trough intrusions.

(Figure 12), within a radius of 10° during all seasons. This radius is much larger than the radius of around 5° found by *Porcù et al.* [2007] for rainfall distribution near a cut-off center in spring and summer seasons. They found as well that convective rain is more concentrated "underneath" the cut-off low, while large-scale forced precipitation was found to the south of its center.

[29] These results also suggest that there is no strong dependency of the frequency of precipitation and convection on the angle of axis inclination (notice that the figures present the accumulated precipitation occurrence, and is not normalized by the number of ULTs). This apparent discrepancy with previous results, e.g., in the Alpine region, can be explained by the fact that our climatology is not area targeted. This means that although there are configurations that are particularly favorable to heavy rainfall in certain locations, our climatology detects troughs anywhere in the Mediterranean basin (not only troughs, say, to the west of the Alps), where other orientations may have a particularly strong effect, and therefore "distributing" the frequency of precipitation among all orientations. For example, *Zangvil et al.* [2003] showed that major rain days occurring at different locations in Israel (south, center and north) are affected by different orientations of the 500hPa geopotential trough axis (∼45°, ∼90°, ∼135°, respectively). If we consider the entire domain as a whole, however, the integrated result is that there is no preference for each of these inclinations, since it produces rain somewhere in the domain.

[30] To have a more complete picture of the dependency of precipitation and convection on the ULT axis inclinations, we calculate the average area of precipitation and convection by dividing the total number of grid points with precipitation or DCT by the total number of grid points of the search domain, and by the total number of events with each axis of inclination. We searched for the relative position where the precipitation and convection are found with respect to the center of the ULT: to the northeast (quadrant 1), to the southeast (quadrant 2), to the southwest (quadrant 3), and to the northwest (quadrant 4). Figures 13 and 14 show the averaged area that precipitation and convection, respectively, covers for each of these quadrants, for each axis inclination. For all inclinations except ∼45°, precipitation and convection cover a larger area and are more frequent in quadrants 1 and 2, while there is lowest coverage for quadrant 4. This quadrant corresponds to the area upstream of the ULT, which is more dominated by subsidence, while downstream of the ULT conditions are favorable for decreased static stability and upward motion [*Hoskins et al.*, 1985]. For ULTs with ∼45° orientation, both

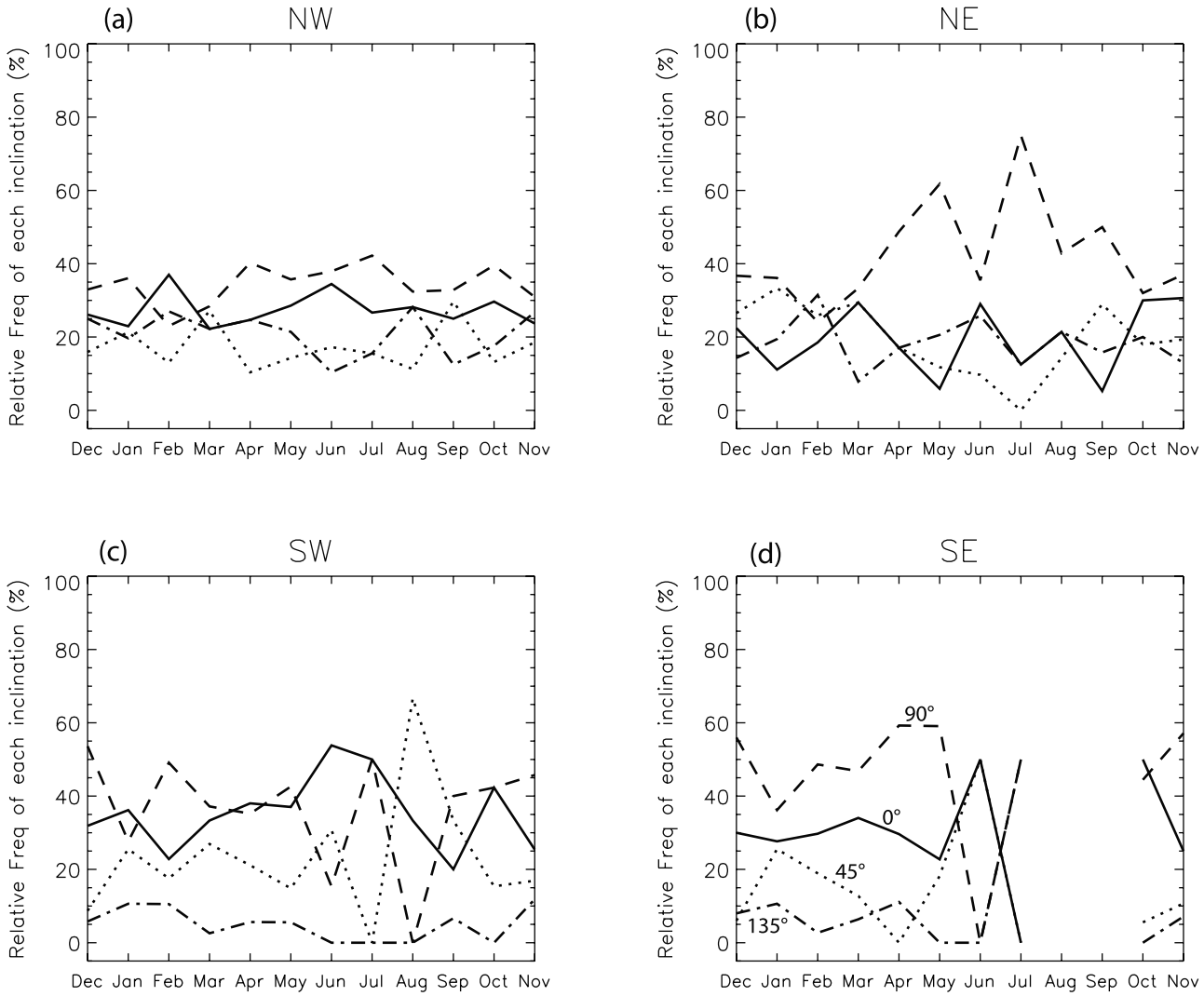

Figure 10. Monthly variation of the number of troughs, according to the angle of axis inclination of the A8 BT′ trough: 0 ([−22.5–22.5°], solid), 45° ([22.5–67.5°], dotted), 90° ([67.5–112.5°], dashed), and 135°([112.5–157.5°], dash-dotted) for NW (a), NE (b), SW (c), and SE (d) regions. Angles relative to the E–W direction.

moderate and convective precipitation is more or less equally distributed between the east (1, 2) and south (3) quadrants.

5. Relationship Between Frequency of ULTs and Large-Scale Atmospheric Circulation

[31] The Mediterranean region is influenced by low-frequency variability modes or patterns in the atmosphere. One such mode is the North Atlantic Oscillation (NAO), the leading mode of winter climate variability in the North Atlantic region [*Hurrel*, 1995; *Rodwell et al.*, 1999]. It consists of a pressure anomaly seesaw with one center located over the North Atlantic between 35–40°N, and another center (with opposite sign) located over Greenland [e.g., *Barnston and Livezey*, 1987]. During the positive phase of the NAO, midlatitude disturbances follow a southwest–northeast oriented storm track, causing more rain in northern Europe and dry conditions over southern Europe. When NAO is negative, there is a decrease in the westerlies, and consequently less warm air off the Atlantic Ocean, causing a build-up of cold and dry air over northern Europe, while southern Europe tends to be wetter than average [*Hurrel*, 1995]. This was observed for example by *Chaboureau and Claud* [2006], who showed that cloud systems in the Mediterranean are more frequent during the negative NAO phase than during the positive phase.

[32] In order to investigate the impact of NAO on the number of ULTs we calculated the correlation between the monthly index of NAO from the US National Weather Service Climate Prediction Center with the anomaly of number of ULTs relative to its average occurrence, from October through March of 2001–2006 (Table 2). During this period, there were 506 days with NAO <0 and 586 days with NAO ≥0. The results showed that the correlation is negative for the northern part of the basin (NW −0.17, NE −0.23) and positive for the southern part (SW 0.41, SE 0.22), significant at more than 90% with the Student's *t*-test in all subdomains except NW. These correlations, being

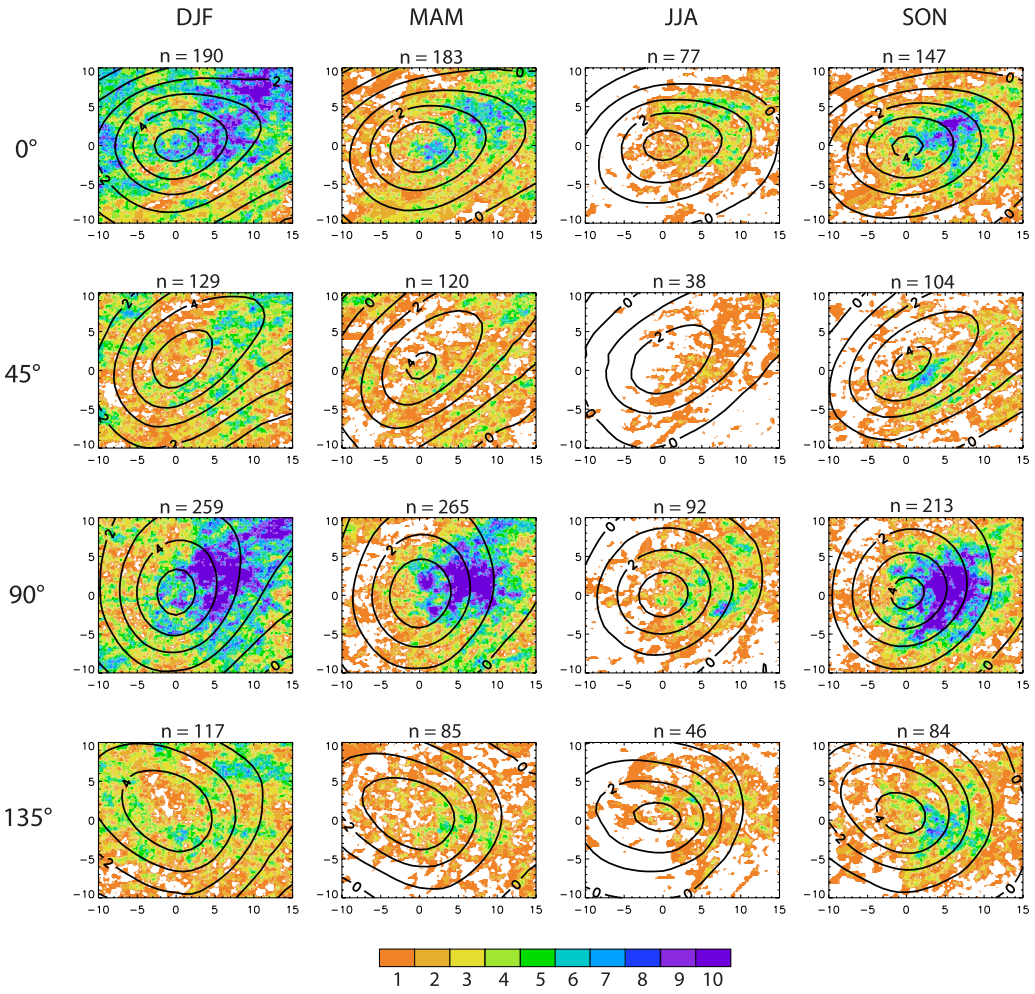

Figure 11. Seasonal spatial distribution for the whole Mediterranean region of total accumulated number of events of rain (shaded) relative to composite of A8 BT′ ULTs (K; contour) with axis inclination marked at the left side for each row. A8 BT′ ULTs are cocentered [in (0,0)] to emphasize axis inclination. Ordinate and abscissa represent the N–S or E–W distances, respectively, in degrees, from the center of composited troughs. *n* represents the total number of troughs, for each inclination and season, to form the composites.

rather weak, indicate that in northeastern part of the domain, when the monthly index of NAO is negative, there is a tendency of more than average occurrences of ULTs, while for the southern part, the opposite is true.

[33] To illustrate this result, we formed composite maps of A8 BT′ for days with contrasted values of NAO, that is, either ≥ 1.5 or ≤ -2, shown in Figure 15. During the negative phase, there is a center of relatively low A8 BT′ placed south of the Balkan peninsula, while the largest A8 BT′ areas are found in the northern part of the domain, where ULTs are concentrated. Conversely, during the positive NAO phase, a relatively high A8 BT′ is found over the eastern Mediterranean Sea, indicating a region of upper-level cyclonic activity. The results obtained are therefore consistent with the corresponding configuration for each phase of the NAO. This result can also be related to those of *Sprenger and Wernli* [2003] who found that stratosphere-to-troposphere exchanges occurs almost exclusively in the positive phase of the NAO in the eastern Mediterranean, and also with *Zangvil et al.* [2003] who found an increase in the occurrence of 500hPa troughs in this NAO phase. Such 500 hPa troughs in the eastern Mediterranean were also found in a canonical correlation analysis pattern describing dynamically a regional manifestation of the NAO known as the Mediterranean Oscillation [*Conte et al.*, 1989], and being positively correlated in wintertime with the NAO [*Dünkeloh and Jacobeit*, 2003].

[34] There are also more occurrences of deep convection in the eastern part of the domain during the positive phase (Figure 15b) of the NAO while in the negative phase (Figure 15a), convection is found more frequently in the western Mediterranean. Despite the fact that we cannot assess the total precipitation amounts, we argue that the number of occurrences of heavy precipitation reflects the wetness or dryness in a certain region because we use a common threshold. That being the case the above results imply that the eastern Mediterranean is wetter in the positive NAO phase than in the negative phase, in agreement with findings of e.g. *Krichak et al.* [2002], *Xoplaki et al.* [2004], and *Krichak and Alpert* [2005]. *Türkes and Erlat* [2005]

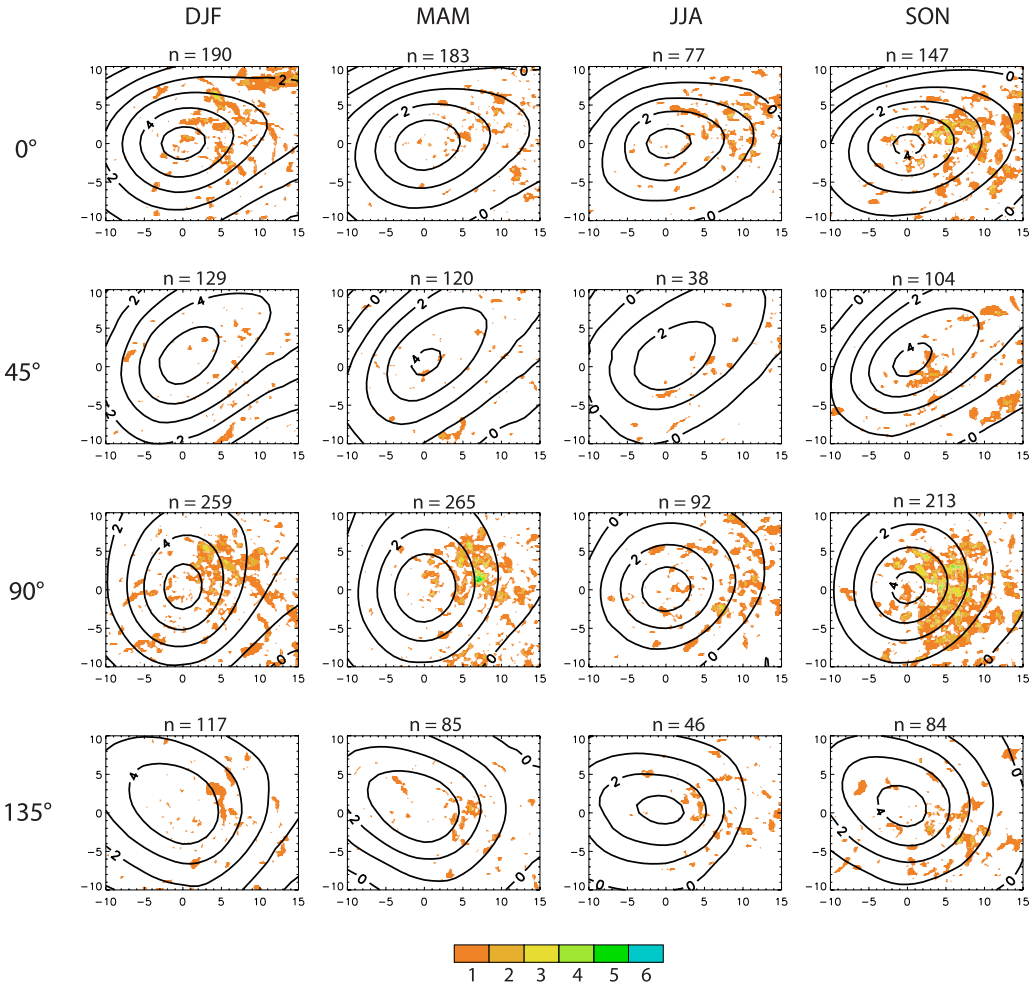

Figure 12. Same as Figure 11 except for the total events of convection.

have found the opposite response for Turkey (i.e., increased/decreased precipitation during negative/positive NAO), but they pointed also that individual strong positive NAO phases tended to cause wet conditions, while strong negative NAO caused severe droughts with widespread spatial coherence.

[35] Other important atmospheric circulation patterns that affect southern Europe and the eastern Mediterranean are the East Atlantic/West Russia (EAWR), East Atlantic (EA) and the Scandinavia (SCA) patterns [*Barnston and Livezey*, 1987]; notice that EAWR and SCA were originally designated as Eurasian patterns types 2 and 1, respectively]. The EAWR pattern comprises three-center east–west pattern, with one center over the North Sea another with equal sign over northeast China, and a center with opposite sign north of the Caspian Sea. The positive phase is characterized by positive 700-hPa height anomalies in the first two locations. This pattern has an important impact on the rainfall distribution in the winter months in Mediterranean, echoing to some degree the NAO response [e.g., *Wibig*, 1999; *Xoplaki et al.*, 2004; *Krichak and Alpert*, 2005]. The East Atlantic pattern comprises a center over the East Atlantic (55°N, 20°–35°W) and "an oppositely signed east-northeast–west-southwest–oriented anomaly band over North Africa or the Mediterranean Sea" [*Barnston and Livezey*, 1987]. This pattern has an important effect on temperature and precipitation variability over the southwestern Europe [e.g., *Sáenz et al.*, 2001], however its effect is negligible in the eastern Mediterranean [*Hasanean*, 2004]. Finally, the SCA pattern has a primary center covering Scandinavia, the Arctic Ocean and north of Siberia, and two weaker centers with opposite signs over western Europe and Mongolia. In its positive phase, there is strong positive pressure anomalies over Scandinavia and western Russia and negative anomaly over the Iberian Peninsula. This blocking-like pattern brings southerlies/southwesterlies over the central Mediterranean and easterlies/southeasterlies over the eastern part of the basin, leading to above-normal precipitation in those regions [e.g., *Corte-Real et al.*, 1995; *Wibig*, 1999]. Unfortunately we are unable to perform the same evaluation for precipitation done for the NAO phases for the EAWR, EA and SCA modes because we do not have the daily indices necessary to perform the composites. Nevertheless, we calculated the correlations between each of these modes and the monthly anomalies of number of ULTs, shown in Table 2. Notice that for the EAWR and EA the period considered is October through March, while for SCA the period is shifted to January through March.

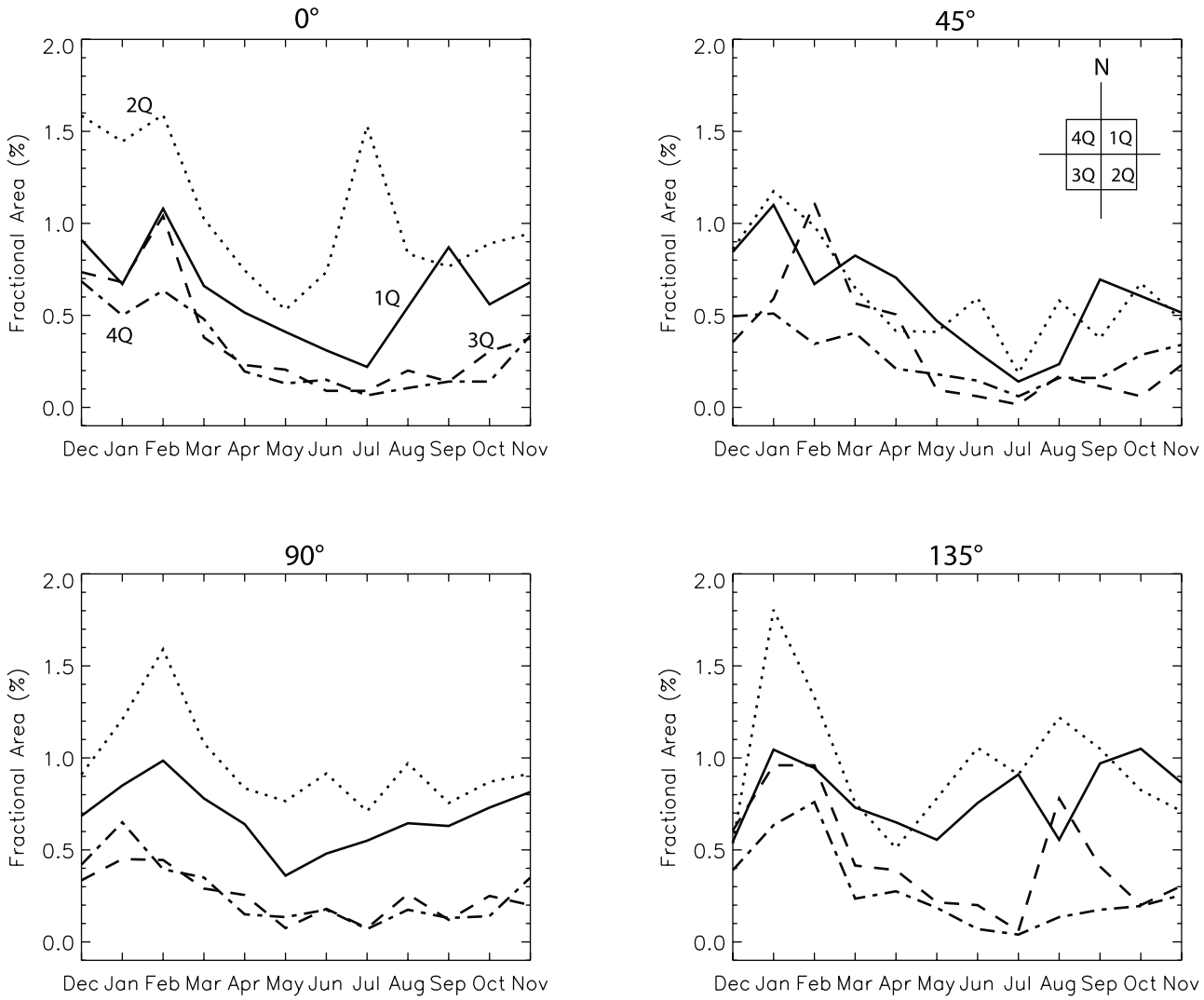

Figure 13. Monthly variation of area of precipitation relative to the center of intrusion (solid, to the NE; dotted, to the SE; dashed, to the SW; and dash-dotted, to the NW), weighted by the total search area and divided by the total number of events, for different axis inclinations: (a) 0°(−22.5–22.5°), (b) 45°(22.5–67.5°), (c) 90°(67.5–112.5°), and (d) 135°(112.5–137.5) Area of search is of 10° north, south and west, and 15° to the east of the center of A8 BT′.

[36] We found that correlations (significant at 90% confidence level) between EAWR and monthly anomalies of number of ULTs are of 0.26 for the SE region, while for the other regions the correlation is negative but not very significant. Therefore the correlations between NAO or EAWR phases and anomalous number of troughs are more significant and resemble each other in the southeastern part of the Mediterranean. For the EA pattern, the correlation is positive for the northern part of the domain and negative for the southern part, showing that its effect is opposite of that of NAO. These results are congruous because the centers of action of the EA pattern are shifted southeastward to the nodal lines of the NAO. Finally for the SCA, there are positive and significant correlation in the NW region (0.29, at 95% significance). This indicates that when there is a blocking high over Scandinavia, there are more intrusions than average in the NW. The same blocking may hinder the propagation of the upper-level troughs eastward causing less than average troughs in the NE region.

6. Summary

[37] We used NOAA-16 AMSU satellite data for the period of January 2001 to December 2006 to form a climatology of ULTs and associated moderate to heavy precipitation over the Mediterranean. ULTs and precipitation are defined at spatial resolutions of 1°lat × 1°lon and 0.2°lat × 0.2°lon, respectively. This is a novel climatology compared with previous studies in two main aspects. First, it is nearly entirely based on direct observations from AMSU, as opposed to earlier studies based mostly on reanalyses. Second, we evaluate the link between intrusions and occurrence of moderate and heavy precipitation, while the majority of studies for the Mediterranean region address the issue in the opposite direction; that is, they examine the

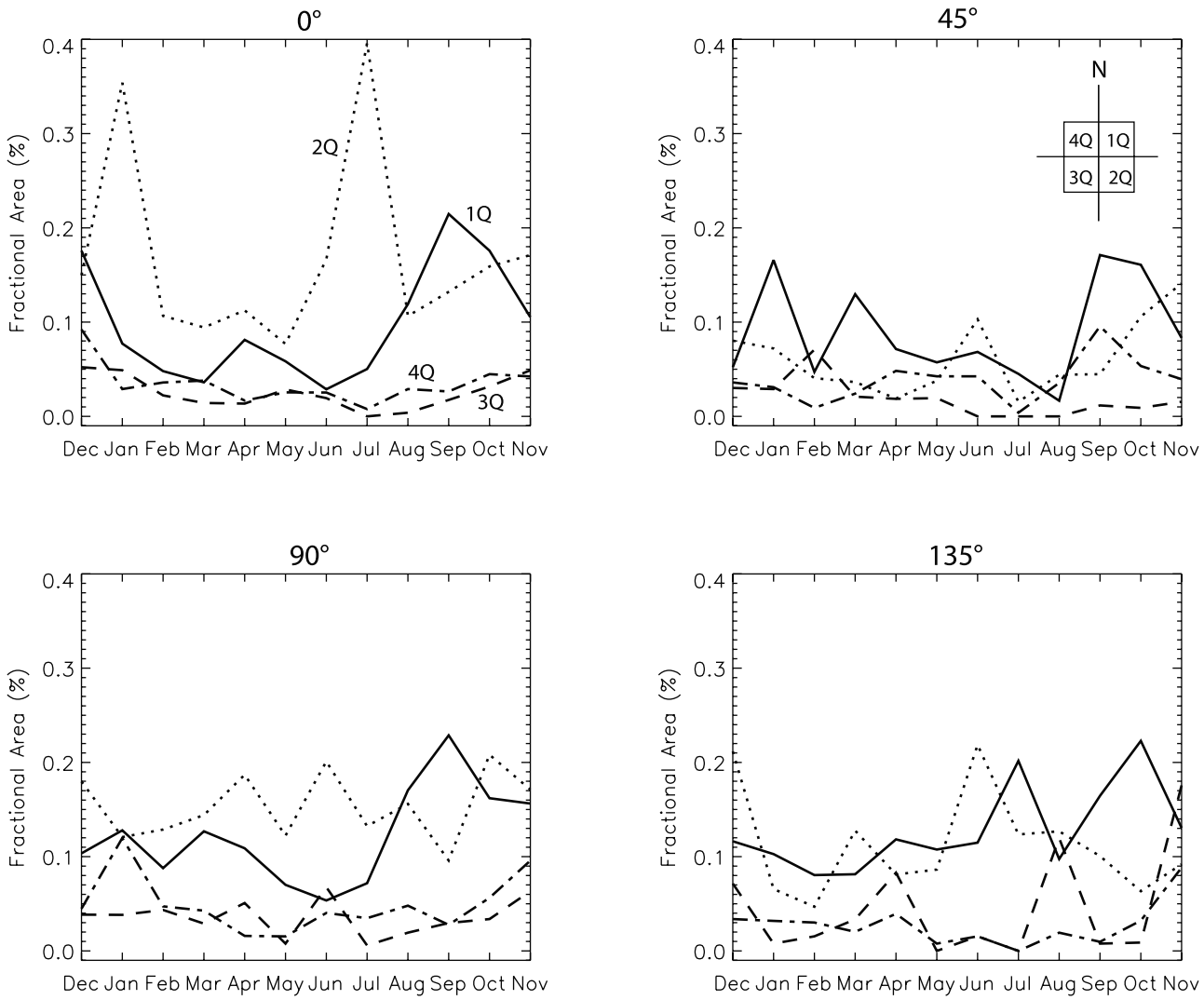

Figure 14. Same as in Figure 13, but for deep convection.

presence of ULTs in the vicinity of a specific region where precipitation occurs. Our main results are summarized below.

[38] We found that ULTs that have a signal of A8 BT′ of at least 3 K are representative of intrusions present in events of heavy precipitation. ULTs that attain this A8 BT′ value are more frequent and/or more persistent in winter than in summer, and they are also larger in size during the cold months. This seasonal behavior can be explained by the shift in the tropopause level as the weighting function of A8 remains nearly stationary; the anomalies are larger in higher levels in the summer and in lower levels in the winter. Therefore in the summer, A8 captures only strong anomalies that penetrate deep vertically into the troposphere. In contrast, the frequency of precipitation (with or without convection) is higher in summer in the NW and NE subdomains, while for the SW and SE the link is nearly of one-to-one throughout the year; that is, whenever an ULT with a signal of A8 BT′ of at least 3 K is present, there is precipitation in the vicinity. This association between ULT and precipitation is very strong in the southern Mediterranean as suggested by the small interannual variability, specially in the SE region, and indicates that precipitation is an ubiquitous feature (in the presence of an ULT) in this area.

[39] An increase in the frequency of convection associated with an ULT is observed toward the summer from relative low values in winter and autumn in all subdomains except SE, where no ULTs were detected in August and September. Our results confirm that summer in SE is characterized by the absence of rain [*Saaroni and Ziv*, 2000; *Tvieli and Zangvil*, 2007] and support the idea that sporadic events are caused by a weakening of the semipermanent inversion at low levels rather by synoptic-scale forcing [*Saaroni and Ziv*, 2000]. The absence of ULTs in the summer in SE can also be attributed to the permanent subsidence associated with the descending branch of the Asian Monsoon [*Rodwell and Hoskins*, 1996; *Ziv et al.*, 2004]. As opposed to moderate precipitation, the interannual variability of convective events in the southern region is very large, and indicates that other factors (such as local topography, surface fluxes) have a large contribution to the triggering of convection. Also, convection may result from tropical intrusions such as the Red Sea Troughs [e.g.,

Table 2. Correlation Coefficients Between Monthly Circulation Indices and Monthly Anomaly of Number of Trough Intrusions for the North Atlantic Oscillation (NAO), East Atlantic/Western Russia (EAWR), East Atlantic (EA), Scinavia (SCA) Patterns[a]

	NAO	EAWR	EA	SCA
NW	−0.17	−0.18	**0.28**	**0.29***
NE	**−0.23**	−0.15	0.13	**−0.15**
SW	**0.41***	−0.11	−0.18	0.10
SE	**0.22**	**0.26**	**−0.24**	−0.08

[a]For all patterns, except SCA, the period considered is October through March, while for SCA the period is January through March. Values in bold are correlations significant at 90% or more according to the Student's *t*-test (starred significant at 95%).

Kahana et al., 2002]. In the northern part of the Mediterranean, the frequency of deep convection is low during the winter and increases in the summer and early autumn. There is interannual variability but it is smaller compared to the variability of moderate precipitation and to the southern part of the domain. On average, in the northern part of the basin 1 out of 5 ULTs in winter yields an event of heavy precipitation, while on summer and early autumn this ratio increases to 3 to 4 out of 5 ULTs. The differences between the north and south Mediterranean in winter may be also explained by the stability changes within the precipitating air masses. These affecting the south are originally cold but warmed from below by the warm Mediterranean sea, releasing conditional instability. For those entering the north, they are either warm and get cooled by the cold continental surface, or are originally continental polar, i.e., stable in both cases.

[40] We found that the ULTs as shown in the A8 BT′ fields have more frequently an axis in the N–S direction, however the dependency of the relative frequency or area coverage of precipitation on the inclination of the ULT was virtually nonexistent. For each ULT, areas of moderate precipitation and/or convection were found to be larger at its leading edge, and concentrated within a radius of

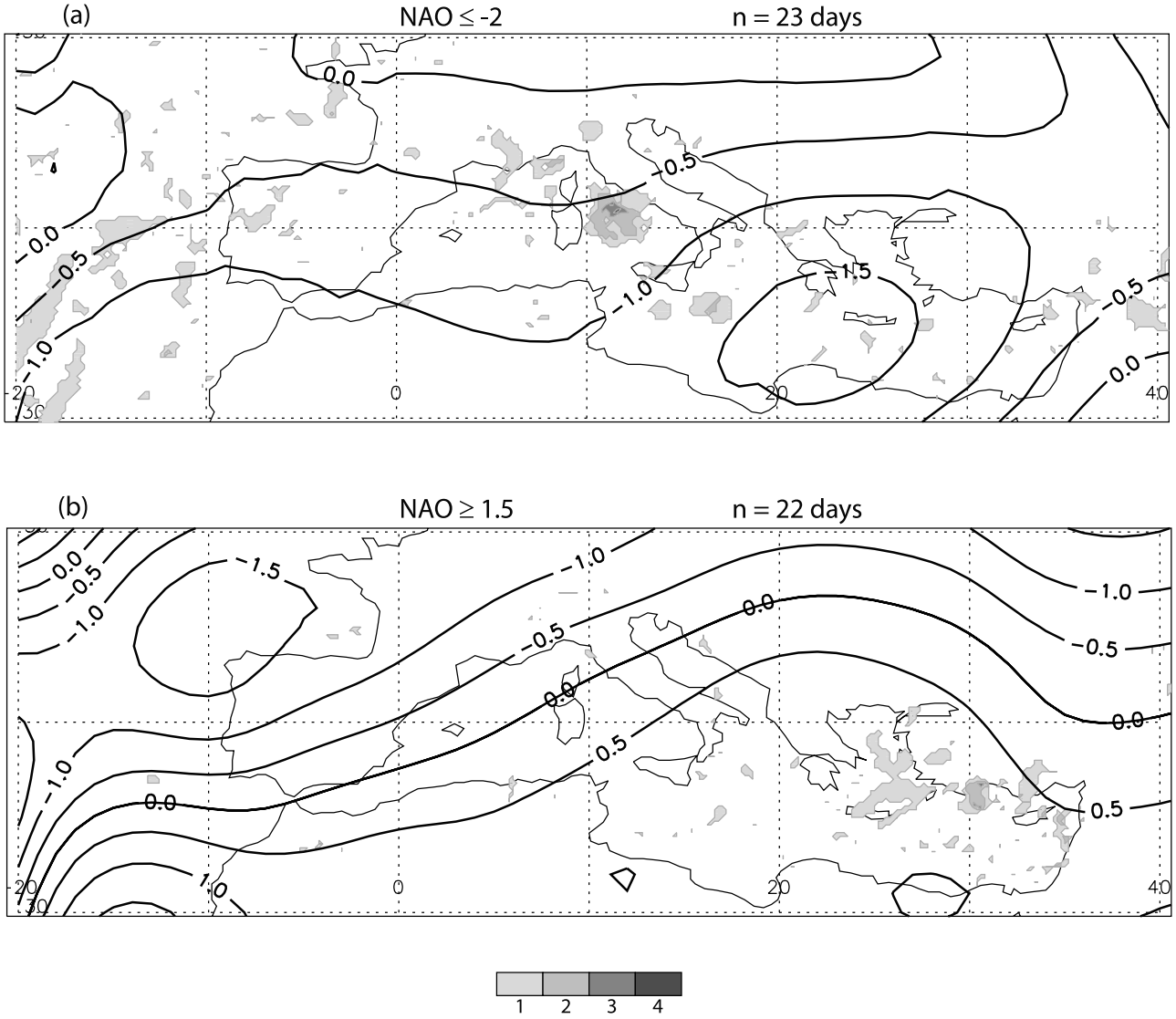

Figure 15. Composites of A8 BT′ (K; contours) and number of occurrences of deep convection (shaded) for negative (≤−2) (a) and positive (≥1.5) (b) NAO indices between October through March 2001–2006.

approximately 10° relative to the center of the intrusion. This radius is double of that found by *Porcù et al.* [2007] for precipitation found near midtropospheric cut-off lows in spring and summer.

[41] In general, the above results were found to be robust relative to the BT' threshold value for ULT detection. We found that increasing the value of BT' from 3 to 4 or 5 K did not change the overall results: There are more ULTs in the NW region than in the other regions (except in March and April, when SW region has slightly higher number than NW), and there is a decrease in the number of ULTS from winter to summer. The absolute decrease in the average number of days with troughs was of around 50% and 75%, for thresholds of $BT' \geq 4$ and 5 K, respectively, compared to $BT' \geq 3$ K for the month of December. As the threshold increases, so does the number of months where such intrusions are not detected, mainly in late spring through early autumn. The associated frequency of precipitation does not change significantly, which is in part explained by the fact that a threshold of 3 K includes anomalies that can be much higher (which happen mostly in the winter), and consequently, the results presented already demonstrate the behavior of anomalies that are stronger than the threshold chosen (up to 5 K). For values of $BT' \gg 3$ K the events are scarcer and more difficult to draw general conclusions.

[42] With respect to the modulation of the frequency of ULTs by the NAO, we found that the correlation between NAO and anomalies in the number of intruding troughs is larger and more significant in the southern Mediterranean (October through March). ULTs are more (less) frequent than average in the northern (southern) part of the basin in years of negative NAO than in its positive phase. These results are consistent with those obtained by *Sprenger and Wernli* [2003] for stratosphere to troposphere intrusions and to *Zangvil et al.* [2003] for 500 hPa troughs, both in the southeastern region. Also, more convective events were found in the eastern (western) part of the Mediterranean during the positive (negative) phase. These overall results are in line with those of *Eshel and Farrel* [2000], *Krichak et al.* [2002], *Xoplaki et al.* [2004], *Krichak and Alpert* [2005], and *Türkes and Erlat* [2005]. We also found that the response of the number of intrusions to another low-frequency variability mode, the East Atlantic/West Russia pattern, is similar to the NAO except for the SW region. The East Atlantic mode, on the other hand, has positive correlation (i.e., more intrusions than average) in the northern part and negative correlation in the southern part of the domain. The Scandinavia pattern has significant positive correlation only in the NW region, but overall more (less) ULTs in the western (eastern) Mediterranean in its positive phase.

[43] Our study presents the first results toward a Mediterranean climatology on the relationship between upper-level troughs and precipitation using direct observations from satellite data. Our results are important in several aspects. First, it provides a guidance (e.g., for forecasting purposes) on the average frequency of troughs for each season and the related precipitation frequency and distribution, giving an indication of expected behavior. Second, it also provides a contribution for climate change detection. Changes in precipitation occurrence and distribution in the Mediterranean region can be related for example to a decrease or increase in the number of intrusions penetrating in the region, for different climate change scenarios. As NOAA 15 to 18 satellites continues in orbit, this database can be increased which will permit to extend these results.

[44] **Acknowledgments.** This study was sponsored by the French Ministry of Research through the project CYPRIM (CYclognenèse et PRécipitation Intenses en région Méditerranéenne). AMSU data was obtained through the French Mixed Service Unit ICARE. The daily and monthly NAO and EAWR/EA/SCA indices were obtained from the National Weather Service Climate Prediction Center site ftp://ftp.cpc.ncep.noaa.gov/wd52dg/data/indices/tele_index.nh. We express our appreciation to three anonymous reviewers for their insightful remarks that have improved the manuscript.

References

Alpert, P., and B. U. Neeman (1990a), Climatological analysis of Mediterranean cyclones using ECMWF data, *Tellus*, *42A*, 65–77.

Alpert, P., and B. U. Neeman (1990b), Intermonthly variability of cyclone tracks in the Mediterranean, *J. Clim.*, *3*, 1474–1478.

Barnston, A. G., and R. E. Livezey (1987), Classification, seasonality and persistence of low-frequency atmospheric circulation patterns, *Mon. Wea. Rev.*, *115*, 1083–1126.

Buehler, S. A., and V. O. John (2005), A simple method to relate microwave radiances to upper tropospheric humidity, *J. Geophys. Res.*, *110*, D02110, doi:10.1029/2004JD005111.

Buehler, S. A., M. Kuvatov, and V. O. John (2005), Scan asymmetries in AMSU-B data, *Geophys. Res. Lett.*, *32*, L24810, doi:10.1029/2005GL024747.

Chaboureau, J.-P., and C. Claud (2003), Observed variability of North Atlantic oceanic precipitating systems during winter, *J. Geophys. Res.*, *108*(D14), 4435, doi:10.1029/2002JD003343.

Chaboureau, J.-P., and C. Claud (2006), Satellite-based climatology of Mediterranean cloud systems and their association with large-scale circulation, *J. Geophys. Res.*, *111*, D01102, doi:10.1029/2005JD006460.

Chaboureau, J.-P., C. Claud, J. P. Cammas, and P. J. Mascart (2001), Large-scale cloud, precipitation, and upper level features during Fronts and Atlantic Storm Track Experiment as inferred from TIROS-N Operational Vertical Sounder observations, *J. Geophys. Res.*, *106*(D15), 17,293–17,302.

Conte, M., A. Giuffrida, and S. Tedesco (1989), The Mediterranean Oscillation: Impact on precipitation and hydrology in Italy, in *Proceedings of the Conference on Climate and Water*, vol. 1, pp. 121–137, Publications of the Academy of Finland, Helsinki, 11–15 September 1989.

Corte-Real, J., Z. Zhang, and X. Wang (1995), Large-scale circulation regimes and surface climatic anomalies over the Mediterranean, *Int. J. Climatol.*, *15*, 1135–1150.

Delrieu, G., et al. (2005), The catastrophic flash-flood event of 8–9 September 2002 in the Gard Region, France: A first case study for the Cévennes-Vivarais Mediterranean Hydrometeorological Observatory, *J. Hydrometeorol.*, *6*, 34–52.

Doswell, C. A., C. Ramis, R. Romero, and S. Alonso (1998), A diagnostic study of three heavy precipitation episodes in the western Mediterranean region, *Wea. Forecast.*, *13*, 102–124.

Ducrocq, V., G. Aullo, and P. Santurette (2003), Les précipitations intenses et les inondations du 12 et 13 novembre 1999 sur le sud de la France, *La Météorlogie, 8th série*, *42*, 18–27.

Ducrocq, V., C. Lebeaupin, T. Thouvenin, and H. Giordani (2004), L'événement des 8–9 Septembre 2002: situation météorologique et simulation á mésoéchelle, *La Houille Blanche*, *6*, 86–92.

Ducrocq, V., O. Nuissier, D. Ricard, C. Lebeaupin, and T. Thouvenin (2008), A numerical study of three catastrophic precipitating events over southern France. Part II: Mesoscale triggering and stationarity factors, *Q. J. R. Meteorol. Soc.*, *134*, 131–145.

Dünkeloh, A., and J. Jacobeit (2003), Circulation dynamics of Mediterranean precipitation variability 1948–98, *Int. J. Climatol.*, *15*, 1843–1866.

Dutton, J. A. (1995), *Dynamics of Atmospheric Motion*, 617 pp, Dover Publications, Inc., Mineola, NY.

Eshel, G., and B. F. Farrell (2000), Mechanisms of eastern Mediterranean rainfall variability, *J. Atmos. Sci.*, *57*, 3219–3232.

Fischer, E. M., S. I. Seneviratne, D. Lüthi, and C. Schär (2007), Contribution of land-atmosphere coupling to recent European summer heat waves, *Geophys. Res. Lett.*, *34*, L06707, doi:10.1029/2006GL029068.

Fourrié, N., C. Claud, and A. Chédin (2003), Depiction of upper-level precursors of the December 1999 storms from TOVS observations, *Wea. Forecast.*, *18*, 417–430.

Frei, C., H. C. Davies, J. Gurtz, and C. Schär (2001), Climate dynamics and extreme precipitation and flood events in Central Europe, *Integrated Assessment*, *1*, 281–299.

Funatsu, B. M., C. Claud, and J.-P. Chaboureau (2007), Potential of advanced microwave sounding unit to identify precipitating systems and associated upper-level features in the Mediterranean region: Case studies, *J. Geophys. Res.*, *112*, D17113, doi:10.1029/2006JD008297.

Giorgi, F. (2006), Climate change hot-spots, *Geophys. Res. Lett.*, *33*, L08707, doi:10.1029/2006GL025735.

Greenwald, T. J., and S. A. Christopher (2002), Effect of cold clouds on satellite measurements near 183 GHz, *J. Geophys. Res.*, *107*(D13), 4170, doi:10.1029/2000JD000258.

Hasanean, H. M. (2004), Wintertime surface temperature in Egypt in relation to the associated atmospheric circulation, *Int. J. Climatol.*, *24*, 985–999.

Hoinka, K. P., C. Schwierz, and O. Martius (2006), Synoptic-scale weather patterns during Alpine heavy rain events, *Q. J. R. Meteorol. Soc.*, *132*, 2860–2953.

Holton, J. R. (1992), *An Introduction to Dynamic Meteorology*, 3rd ed., International Geophysics Series vol. 48, 511 pp, Academic Press, San Diego, CA.

Hong, G., G. Heygster, J. Miao, and K. Klaus (2005), Detection of tropical deep convective clouds from AMSU-B water vapour channels measurements, *J. Geophys. Res.*, *110*, D05205, doi:10.1029/2004JD004949.

Hoskins, B. J., M. E. McIntyre, and A. W. Robertson (1985), On the use and significance of isentropic potential vorticity maps, *Q. J. R. Meteorol. Soc.*, *111*, 877–946.

Hulme, M., E. M. Barrow, N. W. Arnell, P. A. Harrison, T. C. Johns, and T. E. Downing (1999), Relative impacts of human-induced climate change and natural variability, *Nature*, *397*, 688–691.

Hurrell, J. W. (1995), Decadal trends in the North Atlantic oscillation: Regional temperatures and precipitation, *Science*, *269*, 676–679.

Jansà, A., A. Genovés, M. A. Picornell, J. Campins, R. Riosalido, and O. Carretero (2001), Western Mediterranean cyclones and heavy rain: part 2. Statistical approach., *Meteorol. Appl.*, *8*, 43–56.

Jasper, K., and P. Kaufmann (2003), Coupled runoff simulations as validation tools for atmospheric models at the regional scale, *Q. J. R. Meteorol. Soc.*, *129*, 673–692.

Kahana, R., B. Ziv, Y. Enzel, and U. Dayan (2002), Synoptic climatology of major floods in the Negev Desert, Israel, *Int. J. Climatol.*, *22*, 867–882.

Kotroni, V., K. Lagouvardos, E. Defer, S. Dietrich, F. Porcù, C. M. Medaglia, and M. Demirtas (2006), The Antalya 5 December 2002 storm: Observations and model analysis, *J. Appl. Meteorol. Climatol.*, *45*, 576–590.

Krichak, S. O., and P. Alpert (2005), Signatures of the NAO in the atmospheric circulation during wet winter months over the Mediterranean region, *Theor. Appl. Climatol.*, *82*, 27–39.

Krichak, S. O., P. Kishcha, and P. Alpert (2002), Decadal trends of main Eurasian oscillations and the Mediterranean precipitation, *Theor. Appl. Climatol.*, *72*, 209–220.

Krichak, S. O., P. Alpert, and D. Melina (2004), The role of atmospheric processes associated with Hurricane Olga in the December 2001 floods in Israel, *J. Hydrometeorol.*, *5*, 1259–1270.

Lionello, P., et al. (2006), Cyclones in the Mediterranean region: Climatology and effects on the environment, in *Mediterranean Climate Variability*, edited by P. Lionello, P. Malanotte-Rizzoli, and R. Boscolo, pp. 325–372, Elsevier.

Luterbacher, J., M. A. Liniger, A. Menzel, N. Estrella, P. M. Della-Marta, C. Pfister, T. Rutishauser, and E. Xoplaki (2007), Exceptional European warmth of autumn 2006 and winter 2007: Historical context, the underlying dynamics, and its phenological impacts, *Geophys. Res. Lett.*, *34*, L12704, doi:10.1029/2007GL029951.

Martius, O., E. Zenklusen, C. Schwierz, and H. C. Davies (2006), Episodes of alpine heavy precipitation with an overlying elongated stratospheric intrusion: A climatology, *Int. J. Climatol.*, *26*, 1149–1164, doi:10.1002/joc.1295.

Massacand, A. C., H. Wernli, and H. C. Davies (1998), Heavy precipitation on the Alpine southside: An upper-level precursor, *Geophys. Res. Lett.*, *25*(9), 1435–1438.

Nuissier, O., V. Ducrocq, D. Ricard, C. Lebeaupin, and S. Anquetin (2008), A numerical study of three catastrophic precipitating events over southern France: Part I. Numerical framework and synoptic ingredients, *Q. J. R. Meteorol. Soc.*, *134*, 111–130.

Porcù, F., A. Carrassi, C. M. Medaglia, F. Prodi, and A. Mugnai (2007), A study on cut-off low vertical structure and precipitation in the Mediterranean region, *Meteorol. Atmos. Phys.*, *96*, 121–140.

Riosalido, R. (1990), Characterization of mesoscale convective systems by satellite pictures during PREVIMET MEDITERRANEO-89 (in Spanish). Segundo Simposio Nacional de Predicción, Instituto Nacional de Meteorología, Apartado 285, 28071, Madrid, 135-148.

Rodwell, M. J., and B. J. Hoskins (1996), Monsoons and the dynamics of deserts, *Q. J. R. Meteorol. Soc.*, *122*, 1385–1404.

Rodwell, M. J., D. P. Rowell, and C. K. Folland (1999), Oceanic forcing of the wintertime North Atlantic Oscillation and European climate, *Nature*, *398*, 320–323.

Saaroni, H., and B. Ziv (2000), Summer rain episodes in a Mediterranean climate, the case of Israel, climatological-dynamical analysis, *Int. J. Climatol.*, *20*, 191–209.

Sáenz, J., C. Rodriguez-Puebla, J. Fernández, and J. Zubillaga (2001), Interpretation of interannual winter temperature variations over southwestern Europe, *J. Geophys. Res.*, *106*(D18), 20,641–20,651.

Sprenger, M., and H. Wernli (2003), A northern hemispheric climatology of cross-tropopause exchange for the ERA15 time period (1979–1993), *J. Geophys. Res.*, *108*(D12), 8521, doi:10.1029/2002JD002636.

Sprenger, M., H. Wernli, and M. Bourqui (2007), Stratosphere-troposphere exchange and its relation to potential vorticity streamers and cutoffs near the extratropical tropopause, *J. Atmos. Sci.*, *64*, 1587–1602.

Trigo, I. F., T. D. Davies, and G. R. Bigg (1999), Objective climatology of cyclones in the Mediterranean region, *J. Clim.*, *12*, 1685–1696.

Trigo, I. F., G. R. Bigg, and T. D. Davies (2002), Climatology of cyclogenesis mechanisms in the Mediterranean, *Mon. Wea. Rev.*, *130*, 549–569.

Tvieli, Y., and A. Zangvil (2007), Synoptic climatological analysis of Red Sea Trough and non-Red Sea Trough rain situations over Israel, *Adv. Geosci.*, *12*, 137–143.

Turato, B., O. Realeb, and F. Siccardi (2004), Water vapor sources of the October 2000 Piedmont flood, *J. Hydrometeorol.*, *5*, 693–712.

Türkes, M., and E. Erlat (2005), Climatological responses of winter precipitation in Turkey to variability of the North Atlantic Oscillation during the period 1930–2001, *Theor. Appl. Climatol.*, *81*, 45–69.

Vautard, R., P. Yiou, F. D'Andrea, N. de Noblet, N. Viovy, C. Cassou, J. Polcher, P. Ciais, M. Kageyama, and Y. Fan (2007), Summertime European heat and drought waves induced by wintertime Mediterranean rainfall deficit, *Geophys. Res. Lett.*, *34*, L07711, doi:10.1029/2006GL028001.

Walser, A., and C. Schär (2004), Convection-resolving precipitation forecasting and its predictability in Alpine river catchments, *J. Hydrol.*, *288*, 57–73.

Weng, F., L. Zhao, R. R. Ferraro, G. Poe, X. Li, and N. C. Grody (2003), Advanced microwave sounding unit cloud and precipitation algorithms, *Radio Sci.*, *38*(4), 8068, doi:10.1029/2002RS002679.

Wibig, J. (1999), Precipitation in Europe in relation to circulation patterns at the 500 hPa level, *Int. J. Climatol.*, *19*, 253–269.

Xoplaki, E., J. F. González-Rouco, J. Luterbacher, and H. Wanner (2004), Wet season Mediterranean precipitation variability: Influence of large-scale dynamics and trends, *Clim. Dyn.*, *23*, 63–78, doi:10.1007/s00382-004-0422-0.

Yiou, P., R. Vautard, P. Naveau, and C. Cassou (2007), Inconsistency between atmospheric dynamics and temperatures during the exceptional 2006/2007 fall/winter and recent warming in Europe, *Geophys. Res. Lett.*, *34*, L21808, doi:10.1029/2007GL031981.

Zangvil, A., and P. Druian (1990), Upper air trough axis orientation and the spatial distribution of rainfall over Israel, *Int. J. Climatol.*, *10*, 57–62.

Zangvil, A., S. Karas, and A. Sasson (2003), Connection between Eastern Mediterranean seasonal mean 500 hPa height and sea-level pressure patterns and the spatial rainfall distribution over Israel, *Int. J. Climatol.*, *23*, 1567–1576.

Ziv, B., H. Saaroni, and P. Alpert (2004), The factors governing the summer regime of the eastern Mediterranean, *Int. J. Climatol.*, *24*, 1859–1871.

Ziv, B., U. Dayan, Y. Kushnir, C. Roth, and Y. Enzel (2006), Regional and global atmospheric patterns governing rainfall in the southern levant, *Int. J. Climatol.*, *26*, 55–73.

J.-P. Chaboureau, Laboratoire d'Aérologie, University of Toulouse/CNRS, Toulouse, France. (jean-pierre.chaboureau@aero.obs-mip.fr)

C. Claud and B. M. Funatsu, Laboratoire de Meteorologie Dynamique (IPSL/CNRS), Ecole Polytechnique, 91128 Palaiseau CEDEX, France. (chantal.claud@lmd.polytechnique.fr; funatsu@lmd.polytechnique.fr)